Machine learning models to identify patient and microbial genetic factors associated with carbapenem-resistant *Klebsiella pneumoniae* infection

Zena Lapp BA[a], Jennifer H Han MD[b], Jenna Wiens PhD[c], Ellie JC Goldstein MD[d,e], Ebbing Lautenbach MD[f], Evan S Snitkin PhD[g#]

Running title: Patient and microbial predictors of infection

[a]Department of Computational Medicine and Bioinformatics, University of Michigan; 1510A MSRB I, 1150 W. Medical Center Dr., Ann Arbor, MI, 48109-5680

[b]GlaxoSmithKline; 14200 Shady Grove Road, Rockville, MD 20850

[c]Department of Electrical Engineering and Computer Science, University of Michigan; 3765 Beyster, 2260 Hayward Street, Ann Arbor, MI 48109

[d]R M Alden Research Laboratory

[e]David Geffen School of Medicine, University of California, Los Angeles; 2021 Santa Monica Blvd. #640-E, Santa Monica, CA 90404-2208

[f]Department of Medicine (Infectious Diseases), Department of Biostatistics, Epidemiology, and Informatics, Perelman School of Medicine, University of Pennsylvania; 502A Johnson Pavilion, 3610 Hamilton Walk, Philadelphia, PA 19104-6073

[g]Department of Microbiology and Immunology, Department of Internal Medicine/Division of Infectious Diseases, University of Michigan, Ann Arbor, Michigan; 1520D MSRB I, 1150 W. Medical Center Dr., Ann Arbor, MI, 48109-5680

Corresponding author: Evan Snitkin

Address: 1520D MSRB I, 1150 W. Medical Center Dr., Ann Arbor, MI, 48109-5680

Email: esnitkin@med.umich.edu

Telephone: (734) 647-6472

Abstract

Carbapenem-resistant *Klebsiella pneumoniae* (CRKP) is a critical-priority antibiotic resistance threat that has emerged over the past several decades, spread across the globe, and accumulated resistance to last-line antibiotic agents. While CRKP infections are associated with high mortality, only a small subset of patients acquiring CRKP colonization will develop clinical infection. Here, we sought to determine the relative importance of patient characteristics and CRKP genetic background in determining patient risk of infection. Machine learning models classifying colonization vs. infection were built using whole-genome sequences and clinical metadata from a comprehensive set of 331 CRKP isolates collected across 21 long-term acute care hospitals over the course of a year. Model performance was evaluated based on area under the receiver operating characteristics curve (AUROC) on held-out test data. We found that patient and genomic features were predictive of clinical CRKP infection to similar extents (AUROC IQRs: patient=0.59-0.68, genomic=0.55-0.61, combined=0.62-0.68). Patient predictors of infection included the presence of indwelling devices, kidney disease and length of stay. Genomic predictors of infection included presence of the ICEKp10 mobile genetic element carrying the yersiniabactin iron acquisition system, and disruption of an O-antigen biosynthetic gene in a sub-lineage of the epidemic ST258 clone. Altered O-antigen biosynthesis increased association with the respiratory tract, and subsequent ICEKp10 acquisition was associated with increased virulence. These results highlight the potential of integrated models including both patient and microbial features to provide a more holistic understanding of patient clinical trajectories.

Importance

Multidrug resistant organisms, such as carbapenem-resistant Klebsiella pneumoniae (CRKP), colonize alarmingly large fractions of patients in endemic regions, but only a subset of patients develop life-threatening infections. While patient characteristics influence risk for infection, the

52 relative contribution of microbial genetic background to patient risk remains unclear. We used
53 machine learning to determine whether patient and/or microbial characteristics can discriminate
54 between CRKP colonization vs. infection across multiple healthcare facilities and found that
55 both patient and microbial factors were predictive. Examination of informative microbial genetic
56 features revealed features associated with respiratory colonization and higher rates of infection.
57 The methods and findings presented here provide a foundation for future epidemiological,
58 clinical, and biological studies to better understand bacterial infections and clinical outcomes.
59

60 **Introduction**

61

62 Infections due to multidrug resistant organisms lead to hundreds of thousands of deaths
63 worldwide each year (1). Carbapenem-resistant Enterobacterales (CRE) are a critical-priority
64 antibiotic resistance threat that has emerged over the past several decades, spread across the
65 globe, and accumulated resistance to last-line antibiotic agents (2, 3). In the United States
66 (U.S.), CRE infections are primarily caused by the sequence type (ST) 258 strain of
67 carbapenem resistant *Klebsiella pneumoniae* (CRKP), which has become endemic in regional
68 healthcare networks (3–7). In this background of regional endemicity the risk of patient
69 exposure to CRKP is high, as evidenced by alarmingly high rates of colonization, especially in
70 long-term care settings (7, 8). However, even among critically ill patients residing in long-term
71 care facilities, not all colonized patients develop clinical infections that require antibiotic
72 treatment (3, 9). Currently, our understanding of the factors that influence whether a colonized
73 patient develops an infection is incomplete.
74

75 In addition to clinical characteristics of patients, the genetic background of the colonizing strain
76 may also influence the risk of infection, as there is extensive intra-species variation in antibiotic
77 resistance and virulence determinants harbored by *K. pneumoniae* (3). To date, most studies of

78 virulence determinants have been carried out in model systems (10, 11) or examined in human
79 populations without considering patient characteristics or clinical context (11, 12). One recent
80 study investigated virulence determinants in *K. pneumoniae* clinical isolates while controlling for
81 patient characteristics (13). However, this was a single-site study with a focus on carbapenem-
82 susceptible *K. pneumoniae*, thereby not addressing the impact of genomic variation in antibiotic-
83 resistant lineages that circulate in global healthcare systems.
84
85 Here, we sought to understand the importance of both patient factors and CRKP genetic
86 background in determining whether a patient is infected (vs. colonized) with CRKP, and identify
87 a set of patient and microbial features that are consistent predictors of CRKP infection across
88 long-term care facilities. To accomplish this, we compared patients with CRKP colonization and
89 infection based upon both clinical characteristics and the genomes of their colonizing or
90 infecting strains. We leveraged a comprehensive set of all clinical isolates collected from 21
91 long-term acute care hospitals (LTACHs) across the U.S. over the course of a year to obtain an
92 unbiased assessment of the relative contribution of bacterial and host factors to patient
93 colonization and infection with circulating CRKP lineages. To do this, we employed a rigorous
94 machine learning approach that allowed us to perform a direct comparison of patient and
95 bacterial features, as well as identify the most predictive features across our unbiased study
96 population.
97
98 **Results**
99
100 Of 355 clinical CRKP isolates from 21 LTACHs across the U.S. (14), we classified 149 (42%) of
101 the isolates as representing infection based on modified NHSN criteria (**Figure S2**, **Tables S1-**
102 **3**). Stratified by anatomic site, we classified 29/29 (100%) blood isolates as infection, 69/196
103 (35%) respiratory isolates as infection, and 51/130 (39%) urinary isolates as infection (**Table**

104 **S3**). More than 90% of patient isolates were from the epidemic CRKP lineage ST258 (**Tables**
105 **S1**). Patients harboring different sequence types of CRKP showed no significant differences in
106 infection/colonization status or anatomic site of isolation, and no substantive differences in
107 clinical characteristics (see supplementary material). Thus, we decided to limit our analysis to
108 ST258 to improve our ability to discern whether genetic variation within this dominant strain is
109 associated with infection.
110
111 **The CRKP epidemic lineage ST258 shows evidence of sub-lineage variation in virulence**
112 **and anatomic site of isolation**
113 We next evaluated if there exist sub-lineages of ST258 with altered virulence properties by
114 looking for clustering of isolates by infection on the whole-genome phylogeny (**Figure 1**; see
115 supplementary methods) (38). Infection status was non-randomly distributed on the phylogeny
116 (p=0.002), supporting our hypothesis that the genetic background of CRKP influences infection.
117 We performed a similar clustering analysis to look at potential niche-specific adaptation to
118 certain anatomic sites (**Figure 1**), and found that respiratory (p=0.001) and urinary (p=0.013)
119 isolates cluster on the phylogeny, but blood isolates do not (p=0.21). This analysis indicates
120 that, in addition to patient features, intra-strain variation in virulence and adaptation to the
121 urinary and respiratory tract might influence whether patients develop an infection.
122
123 **Both patient and CRKP genetic characteristics are weakly predictive of infection, with**
124 **relative performance being highly facility-dependent**
125 We next performed machine learning to quantify the ability of patient and microbial genetic
126 characteristics to predict CRKP infection (**Figure S1**). To prevent over- or under-fitting and
127 control for facility-level biases, we generated 100 train/test data splits, wherein a given LTACH
128 was only included either in the train or test set. Each LTACH occurred a median of 24 times
129 (range 13-32) in the test data split. In this way, we were able to identify patient and CRKP strain

130 characteristics consistently associated with infection or colonization across data splits, and thus
131 across patient populations in different healthcare facilities.
132
133 First, we sought to understand if patient and genomic features were individually predictive of
134 CRKP infection. To this end, we independently evaluated patient characteristics as well as three
135 different genomic feature sets for their ability to classify colonization and infection. The three
136 genomic feature sets were uncurated genomic (including SNPs, indels, IS elements, and
137 accessory genes), uncurated grouped genomic (variants grouped into genes, akin to a burden
138 test, e.g (28)), and curated genomic (features identified using Kleborate (16)). Across the 100
139 different train/test splits, we observed that the average predictive performance was weak, with
140 each of the genomic and patient feature sets predictive of infection to a similar degree (all 1st
141 quartile AUROCs > 0.5; median range=0.55-0.68; **Figure 2A**; AUPRC: **Figure S3A**).
142 Additionally, no one feature set was consistently the most predictive (e.g. **Figures 2B**, **2C**; all
143 comparisons $p > 0.30$, see supplementary methods for p-value calculation). Furthermore, for
144 each feature set the AUROCs were distributed such that the test AUROC ranged from below
145 0.5 to over 0.7, depending on how the data were split (i.e., which facilities appear in the
146 train/test sets). This variation in model performance across different train/test sets suggests that
147 the association of CRKP strain and patient characteristics with infection or colonization varies
148 across facilities.
149
150 **Integration of patient and CRKP strain features does not improve discriminative**
151 **performance of overall or anatomic site-specific models**
152 To determine if the predictive power of patient and genomic features is additive, and if
153 combining these disparate feature sets improved validation on held-out facilities, we built
154 models including both patient and curated genomic features. The discriminative performance of
155 the models based on the combined feature set was not significantly greater than that of the

156 individual feature sets (**Figure 2A**, $p \geq 0.20$). Thus, despite variation in the predictive capacity of
157 genomic and patient features across facilities (**Figure 2C**), combining the two sets did not
158 improve overall performance. Focusing on anatomic site-specific models revealed similar
159 trends, where classification performances were similar for respiratory and urinary specific
160 models, and the relative predictive capacity of patient and CRKP strain features varied across
161 facility subsets (**Figure S4**; AUPRC: **Figure S3B**).
162
163 **Some patient and genomic features consistently discriminate colonization and infection**
164 After evaluating the predictive capacity of models, we next sought to identify patient and CRKP
165 strain characteristics that are most associated with CRKP infection or colonization. To this end,
166 we identified those patient and genomic features that consistently improved model performance
167 across the 100 different data splits (see methods). Evaluating the importance of features in this
168 way provides insight into those characteristics that generalize across different facility subsets.
169 This approach was taken for both overall and anatomic site-specific models to identify features
170 predictive of different anatomic sites of infection (**Figure 3**, **Figures S5-7**).
171
172 Several patient features were consistently associated with infection in the overall analysis,
173 including presence of a gastrostomy tube, presence of a central venous catheter, acute kidney
174 injury, and severe chronic kidney disease (**Figure 3**), all markers of critically ill patients. Only a
175 small number of genomic features were consistently associated with infection (**Figure 3**). No
176 known virulence factors were positively associated with colonization; all of the genomic features
177 positively associated with colonization are antibiotic resistance elements. Conversely, all but
178 one of the genomic features positively associated with infection (3/4) are related to virulence.
179 The ICEKp10 element is positively associated with infection and carries colibactin and two
180 different types of yersiniabactin, a previously identified *K. pneumoniae* virulence determinant
181 (12) (**Figure S8**). Additionally, insertion sequence-mediated disruption of the O-antigen

182 biosynthetic gene *kfoC* (see supplementary methods and **Figure S9** for insertion sequence
183 identification (21, 23, 39–41)) was associated with respiratory infection. Colibactin is a toxin (3),
184 and yersiniabactin is an iron scavenging system that has been identified in previous animal and
185 human studies as being associated with virulence (3, 10). The O-antigen of lipopolysaccharide
186 (LPS) is a known antigenic marker, although association with a specific anatomic site has not
187 been noted (42).
188
189 **A sub-lineage of ST258 clade II appears to have sequentially evolved enhanced**
190 **adaptation for the respiratory tract and increased virulence**
191 We noted that *kfoC* disruption is largely confined to a sub-lineage of ST258 present across 12
192 LTACHs in California (**Figures 4**, **S10**, **S11**). Consistent with this feature being associated with
193 respiratory infection, the disrupted *kfoC* lineage is enriched in respiratory isolates (82/118, 69%
194 of isolates in the disrupted *kfoC* lineage are respiratory isolates vs. 101/213, 47% in all other
195 isolates; Fisher's exact p=0.0001), suggesting that this lineage is associated with increased
196 capacity for respiratory colonization. Furthermore, a subset of isolates in the disrupted *kfoC* sub-
197 lineage harbor the ICEKp10 element containing yersiniabactin. Examination of these genetic
198 events in the context of the whole-genome phylogeny revealed that disruption of *kfoC* occurred
199 first, followed by at least two different acquisitions of ICEKp10 (**Figures 4**, **S10**). Within the
200 disrupted *kfoC* lineage, isolates with ICEKp10 are enriched in infection (31/55, 56% of isolates
201 with ICEKp10 are infection isolates vs. 16/63, 25% of isolates without ICEKp10, Fisher's exact p
202 = 0.00065), supporting an increase in virulence after acquisition of ICEKp10. It is important to
203 note that the observed clinical associations with ICEKp10 and kfoC disruption do not
204 demonstrate causality, as we cannot rule out the role of correlated genetic variation.
205
206

207 **Discussion**

208 There have been numerous studies aimed at identifying risk factors for healthcare-associated
209 infections caused by prominent antibiotic-resistance threats. For the most part, these studies
210 have found the dominant risk factors to be linked to the magnitude of exposure (e.g. length of
211 stay or colonization pressure), use of antibiotics, and overall comorbidity (43). Here we found
212 similar results, where length of stay and having certain comorbidities were positively associated
213 with infection. What remains unclear is, in the critically ill populations heavily exposed to
214 antibiotics that are at greatest risk, if genetic variation in circulating resistant lineages influences
215 patient infection status. Here, we addressed this question by focusing on CRKP infection in a
216 comprehensively sampled cohort of patients from 21 LTACHs across the U.S. To gain a realistic
217 assessment of the predictive capacities of patient and CRKP genetic features, we employed a
218 machine learning framework using multiple facility-level train/test splits. Overall, we found that,
219 while neither patient nor CRKP genetic features have high predictive accuracy on held-out test
220 data, both feature sets were independently associated with infection, with one or the other being
221 more predictive on different facility subsets. Moreover, the integration of clinical and genomic
222 data led to the discovery of an emergent sub-lineage of the epidemic ST258 clone that may
223 have increased adaptation for the respiratory tract, and is more strongly associated with
224 infection.

225

226 One strength of our machine learning approach is that we were able to measure the variation in
227 discriminative performance across 100 train/test iterations that differed in which facilities were
228 included in train and test sets. We found that performance varied greatly depending on how
229 facilities were allocated to train and test sets, highlighting how smaller studies could
230 overestimate or underestimate the discriminative ability of both their model and individual
231 features. Variation in model performance across facilities could be due to facility-level
232 heterogeneity leading to differences in the prevalence of predictive patient or genomic features

233 in the different test sets. For instance, certain facilities may have patient populations skewed
234 towards individuals with characteristics that are predictive of infection. Alternatively, certain
235 geographic regions may have CRKP strains that are more virulent than in other regions. These
236 differences could lead to a higher predictive power for certain facilities compared to others.
237 Another possible explanation for variation in model performance is that the critically-ill nature of
238 LTACH patients may be such that most patients are actually highly susceptible to infection (i.e.
239 many patients colonized with CRKP may ultimately develop an infection). However, it is
240 noteworthy that despite these potential challenges in creating generalizable models, our
241 analysis did yield predictors of infection and colonization consistent across test sets, and thus
242 across LTACHs.
243
244 We built classifiers including all genomic features as well as a curated subset of features from
245 Kleborate (16), and found that both are similarly weakly predictive of infection. However, while
246 the uncurated feature set presented challenges with downstream interpretation, our analyses on
247 the curated genomic features (16) facilitated novel insights into potential evolutionary
248 trajectories of anatomic site-specific adaptation and virulence. For example, we observed that
249 disruption of the O-antigen biosynthetic gene, *kfoC*, is associated with isolation from the
250 respiratory tract. While we cannot determine from our machine learning analysis if disruption of
251 *kfoC* is directly causal, the biological plausibility of an altered O-antigen structure mediating
252 evasion of innate immunity and/or other beneficial interactions with the host makes this a strong
253 candidate for follow-up experiments. Supporting this hypothesis, a previous study found that
254 absence of O-antigen is associated with decreased virulence, but not decreased intrapulmonary
255 proliferation, in a murine model (44). In addition, we noted that a number of antibiotic resistance
256 determinants were associated with colonization. We hypothesize that this observation could be
257 a consequence of longer duration of residence being associated with increased exposure to off-
258 target antibiotics (45). Finally, we also saw evidence that, after acquiring the virulence factors

259 yersiniabactin and colibactin on the ICEKp10 element, the disrupted *kfoC* subclade became
260 more strongly associated with infection, supporting the idea that circulating ST258 sub-lineages
261 can evolve to become both hypervirulent and multi-drug resistant (19, 46–48).
262
263 It is important to note that the machine learning method we employed does not correct for
264 microbial population structure. We chose this method instead of alternative bacterial genome-
265 wide association methods because our primary interest was in quantifying the overall predictive
266 capacity of bacterial genotype in a patient population that was collected in a comprehensive and
267 unbiased manner (i.e. all clinical isolates from 21 facilities over one year). While alternative
268 methods controlling for population structure may yield more precise estimates of the contribution
269 of individual variants, this would obfuscate the realized contribution in our patient population and
270 hinder direct comparison to the predictive capacity of patient features. However, this then
271 presented the challenge of interpreting our finding that certain sub-populations of CRKP may
272 differ in their predilection for causing infections at different sites. For instance, the *kfoC*
273 disruption is a lineage defining variant, and in principle other variants that define this lineage
274 could also be causal. Here, we limited our analysis to a curated set of variants belonging to
275 pathways known to be associated with antibiotic resistance and virulence, and found that only
276 *kfoC* disruption was associated with increased respiratory infection, thus making it a strong
277 candidate for follow-up in in vitro or in vivo models (10). To identify novel loci whose role in
278 human infection may not be appreciated both computational and experimental strategies may
279 be employed to help prioritize putative causal versus passenger variants. Computationally,
280 investigators may search for evidence of parallelism in genotype/phenotype associations, which
281 would bolster confidence in causality (49). Alternatively, high-throughput screens of genetic
282 mutants in relevant model systems can help prioritize candidates. Garnering further genomic or
283 experimental support for the direct role of a specific genetic variant would in turn increase the
284 likelihood that those genetic markers would be predictive in new strains and patient populations.

285

286 Our study also has several important limitations related to the data available. Specifically, CRKP
287 colonization vs. infection for non-bloodstream isolates may be difficult to discriminate using
288 surveillance criteria and the clinical data that were available. However, we based our definitions
289 on established CDC criteria with modifications used previously (7). Encouragingly, we were still
290 able to identify consistent predictors of infection, even with potential misclassifications. A
291 second limitation is that our dataset only included one clinical culture for the majority of patients,
292 meaning that we were unable to investigate clinical or genomic features that may be associated
293 with progression from colonization to infection. Furthermore, we do not have CRKP rectal
294 colonization isolates, and therefore cannot evaluate transition from rectal colonization to other
295 body sites. However, we hypothesize that comparing rectal colonization to infection may be
296 asking a subtly distinct question - namely bacterial genetic factors that enable translocation from
297 the gut to other body sites. In contrast, we hypothesize that our study design is ideal to identify
298 bacterial genetic factors associated with infection once at a given body site. Additionally, we
299 chose to focus our analysis on ST258 due to its disproportionate presence in our dataset, but
300 this makes it possible that our findings may not generalize to other sequence types.
301 Nevertheless, ST258 is the dominant clone in the U.S., and the methods we employed here can
302 be used to study other sequence types and other pathogens. Furthermore, our focus on the
303 ST258 lineage led to the particularly notable finding that even within an established endemic
304 multi-drug resistant lineage (that emerged circa 2000 (14)), there is continued evolution that
305 influences the manifestation and outcome of infection. We were also limited in the patient data
306 included in our model. It is likely that important differences in underlying patient conditions were
307 not captured by the coarse clinical variables we included, and we also did not account for
308 differences in genetic variation in the host (50). Other limitations include that our study was
309 restricted to LTACH patients, and had non-random geographic sampling. While LTACHs have
310 unique structural features, based on prior studies, we expect that the types of patient risk factors

311 considered are likely to generalize to other patient populations. Moreover, our restriction to
312 LTACHs in endemic geographic regions has the benefit of focusing on populations at
313 disproportionate risk for CRKP infection (8).
314
315 In conclusion, we employed a machine learning approach to quantify our ability to discriminate
316 between CRKP colonization and infection using patient and microbial genomic features. This
317 approach highlighted the high degree of variation in predictive accuracy across different facility
318 subsets. Furthermore, despite modest predictive power, we identified several genomic features
319 consistently associated with infection, indicating that variation in circulating CRKP strains
320 contributes to infection, even in the context of the critically-ill patient populations residing in
321 LTACHs. Future work should aim to corroborate our findings with larger cohorts, and follow up
322 on strong associations to determine whether they are indeed risk factors for infection. This could
323 ultimately help identify patients at high risk for infection and devise targeted strategies for
324 infection prevention.
325

326 Materials & Methods

327

328 Clinical and genomic data

329 We used whole-genome sequences of clinical (non-surveillance) CRKP isolates and associated
330 patient metadata from a prospective observational study performed in 21 LTACHs from across
331 the U.S. over the course of a year (BioProject accession no. PRJNA415194) (14). We included
332 only the first clinical bloodstream, respiratory, or urinary isolate from each patient (n=355;
333 **Figure S1A**), and subset to only ST258 isolates for the majority of analyses (n=331; **Table S1**;
334 see supplementary material for reasoning). Details about the analysis pipeline (15) genomic
335 data curation (14, 16–22), and phylogenetic reconstruction (23–26) are provided in the
336 supplementary material. While most clinical data cannot be shared, the deidentified patient ID,

337 hospital of sample isolation, and isolation site are included in the Sequence Read Archive
338 metadata for the BioProject.
339
340 **Outcome definition**
341 Our outcome of interest was colonization vs. clinical infection (**Figure S1B**). Based on the U.S.
342 Centers for Disease Control and Prevention's (CDC) established National Healthcare Safety
343 Network (NHSN) surveillance definitions, we considered all bloodstream isolates as
344 representative of infection, and used modified definitions to classify urinary and respiratory
345 cultures as representative of infection versus colonization (**Table S2**) (7, 27). Any isolate that
346 did not meet the criteria for infection was classified as colonization.
347
348 **Feature sets**
349 We studied the association between five different feature sets and infection/colonization in
350 CRKP ST258 (**Figure S1C**); the feature sets are described below. See supplementary methods
351 for details on feature set creation and processing. Counts below are for confident features from
352 the entire dataset prior to subsetting for different analyses.
353
354 *Patient:* Clinical features described in Han *et al.* (n=50; **Table S3**) (14).
355 *Uncurated genomic:* Single nucleotide variants, indels, insertion sequence elements, and
356 accessory genes (n=2447).
357 *Uncurated grouped genomic:* Variants grouped into genes (i.e. a burden test, e.g. (28)) and
358 accessory genes (n=3159).
359 *Curated genomic:* Features identified by Kleborate (16), a tool designed to identify the presence
360 of various genes and mutations known to be associated with either CRKP virulence or antibiotic
361 resistance (n=91).
362 *Patient & curated genomic:* Patient features and curated genomic features (n=141).

363

364 **Machine learning & model selection**

365 We aimed to classify clinical infection (vs. colonization) using each of the different feature sets
366 (see above); we built classifiers using the first clinical isolate from each patient for all isolates,
367 only respiratory isolates, and only urinary isolates. We performed L2 regularized logistic
368 regression using a modified version of the machine learning pipeline presented in Topçuoğlu *et*
369 *al.* (29) using caret version 6.0-85 (30) in R version 3.6.2 (31) (**Figure S1D1**). We randomly split
370 the data into 100 unique ~80/20 train/test splits, keeping all isolates from each LTACH grouped
371 in either the training set or the held-out test set to control for facility-level differences among the
372 isolates (e.g., background of circulating strains within each facility, patient population, and
373 clinician test ordering frequency). For valid comparison, the train/test splits were identical across
374 models generated with different feature sets. Hyperparameters were selected via cross-
375 validation on the training set to maximize the average AUROC across cross-validation folds.
376 See supplementary methods for more details.

377

378 **Model performance**

379 We measured model performance using the median test area under the receiver operating
380 characteristic curve (AUROC) and area under the precision recall curve (AUPRC), as well as
381 the interquartile range, across all 100 train/test splits (**Figure S1D2**).

382

383 **Features consistently associated with colonization or infection**

384 To determine the importance of each feature in predicting colonization vs. infection, we
385 measured how much each feature influenced model performance by calculating feature
386 importance using a permutation test (29) (**Figure S1D3**). For each combination of feature and
387 data split, we randomly permuted the feature and calculated the 'permuted test AUROC' using
388 the model generated with the training data. Features with a correlation of 1 were permuted

together. We performed this permutation test 100 times for each feature/data split pair, and obtained a mean feature importance for each data split. A mean feature importance above zero indicates that that feature improved model performance for that data split. We highlight features where the mean permuted test AUROC was above zero in at least 75% of the data splits. In this way, the permutation importance method allows us to take into account the variation we observe across the 100 models, which is not possible with standard parametric statistical tests or odds ratios.

Data analysis & visualization

See supplementary material for details on data analysis and visualization in R version 3.6.2 (31–37). All code and data that is not protected health information is on GitHub (https://github.com/Snitkin-Lab-Umich/ml-crkp-infection-manuscript).

Acknowledgements

We gratefully acknowledge Kindred Healthcare for their assistance in collecting data and isolates used in this study. We also thank Sean Muldoon, MD for his support and guidance throughout the study. Finally, we thank the patients and staff of the long-term acute-care hospitals (LTACHs) for their gracious participation in this study, Begüm Topçuoğlu for help with the machine learning pipeline, Ali Pirani for bioinformatics support, and members of the Snitkin lab, Mike Bachman, and Robert Weinstein for critical review of the manuscript.

Competing interests

JHH was employed at the University of Pennsylvania during the conduct of this study. She is currently an employee of, and holds shares in, the GSK group of companies. All other authors declare that they have no competing interests.

Funding

This research was supported by a CDC Cooperative Agreement FOA #CK16-004-Epicenters for the Prevention of Healthcare Associated Infections, and the National Institutes of Health R01 AI139240-01 and 1R01 AI148259-01. ZL received support from the National Science Foundation Graduate Research Fellowship Program under Grant No. DGE 1256260. Any opinions, findings, and conclusions or recommendations expressed in this material are those of the authors and do not necessarily reflect the views of the National Science Foundation. The funding bodies had no role in the design of the study or collection, analysis, and interpretation of data, or in writing the manuscript.

Authors' contributions

ESS, JHH, EL, and ZL conceptualized the study and acquired funding to support the project. JHH and ZL performed data curation. ZL performed formal analysis, investigation, and visualization. ESS, JW, and ZL developed methodology. ESS supervised the project. ZL and ESS wrote the original draft. All authors reviewed and edited the manuscript.

References

1. Organization WH. 2014. Antimicrobial Resistance: Global Report on Surveillance. World

438 Health Organization, Geneva.
439 2. Munoz-Price LS, Poirel L, Bonomo RA, Schwaber MJ, Daikos GL, Cormican M, Cornaglia
440 G, Garau J, Gniadkowski M, Hayden MK, Kumarasamy K, Livermore DM, Maya JJ,
441 Nordmann P, Patel JB, Paterson DL, Pitout J, Villegas MV, Wang H, Woodford N, Quinn
442 JP. 2013. Clinical epidemiology of the global expansion of Klebsiella pneumoniae
443 carbapenemases. Lancet Infect Dis 13:785–796.
444 3. Wyres KL, Lam MMC, Holt KE. 2020. Population genomics of Klebsiella pneumoniae.
445 Nature Reviews Microbiology 1–16.
446 4. Ansari U, Lawsin A, Campbell D, Albrecht V, McAllister G, Bulens S, Walters MS, Jacob
447 JT, Satola SW, Wilson LE, Lynfield R, Vagnone PMS, Janelle SJ, Xavier K, Dumyati G,
448 Hardy D, Phipps EC, Culbreath K, Beldavs Z, Morey K, Kainer MA, Roberts S, Kallen A,
449 Rasheed JK, Karlsson MS. 2017. Molecular Characterization of Carbapenem-Resistant
450 Enterobacteriaceae in the USA, 2011–2015. Open Forum Infect Dis 4:S179–S179.
451 5. Logan LK, Weinstein RA. 2017. The Epidemiology of Carbapenem-Resistant
452 Enterobacteriaceae: The Impact and Evolution of a Global Menace. J Infect Dis 215:S28–
453 S36.
454 6. Lee C-R, Lee JH, Park KS, Kim YB, Jeong BC, Lee SH. 2016. Global Dissemination of
455 Carbapenemase-Producing Klebsiella pneumoniae: Epidemiology, Genetic Context,
456 Treatment Options, and Detection Methods. Front Microbiol 7.
457 7. Han JH, Goldstein EJC, Wise J, Bilker WB, Tolomeo P, Lautenbach E. 2017. Epidemiology
458 of Carbapenem-Resistant Klebsiella pneumoniae in a Network of Long-Term Acute Care
459 Hospitals. Clin Infect Dis 64:839–844.
460 8. Lin MY, Lyles-Banks RD, Lolans K, Hines DW, Spear JB, Petrak R, Trick WE, Weinstein
461 RA, Hayden MK, Acuna N, Albright R, Alexander P, Anthony T, Bardowski L, Berends C,
462 Bonebrake A, Bova J, Braggs A, Burtun S, Byrnes MA, Cagle C, Chavis R, Cienkus S,
463 Collins-Johnson S, Coomer C, Chou T, Cullen D, DeGuzman D, Donceras O, Feller M,

464 Fung S, Gasienica JAM, Garcia-Houchins S, Genovese G, Gentile M, Gonzaga G,
465 Goodwin E, Hernandez E, Kerridge J, Kirk J, Lavin MA, Lee S, Lepinski J, Myrick S, Oats
466 T, O'Donnell A, Pasinos V, Patton JA, Perez M, Purpura J, Rakoski L, Reiner S, Saiyed A,
467 Santine M, Schmitt B, Schultz C, Semar RM, Sethuraman H, Silkaitis C, Stutler E,
468 Thompson A, Wickman K, Bolon M, Cha A, Landon E, Malow J, Mohapatra S, Segreti J,
469 Weber S, Welbel S, Zembower T. 2013. The Importance of Long-term Acute Care
470 Hospitals in the Regional Epidemiology of Klebsiella pneumoniae Carbapenemase–
471 Producing Enterobacteriaceae. Clin Infect Dis 57:1246–1252.
472 9. Lee BY, Bartsch SM, Wong KF, Kim DS, Cao C, Mueller LE, Gussin GM, McKinnell JA,
473 Miller LG, Huang SS. 2019. Tracking the spread of carbapenem-resistant
474 Enterobacteriaceae (CRE) through clinical cultures alone underestimates the spread of
475 CRE even more than anticipated. Infection Control & Hospital Epidemiology 40:731–734.
476 10. Bachman MA, Oyler JE, Burns SH, Caza M, Lépine F, Dozois CM, Weiser JN. 2011.
477 Klebsiella pneumoniae Yersiniabactin Promotes Respiratory Tract Infection through
478 Evasion of Lipocalin 2. Infection and Immunity 79:3309–3316.
479 11. Ernst CM, Braxton JR, Rodriguez-Osorio CA, Zagieboylo AP, Li L, Pironti A, Manson AL,
480 Nair AV, Benson M, Cummins K, Clatworthy AE, Earl AM, Cosimi LA, Hung DT. 2020.
481 Adaptive evolution of virulence and persistence in carbapenem-resistant Klebsiella
482 pneumoniae. 5. Nature Medicine 26:705–711.
483 12. Holt KE, Wertheim H, Zadoks RN, Baker S, Whitehouse CA, Dance D, Jenney A, Connor
484 TR, Hsu LY, Severin J, Brisse S, Cao H, Wilksch J, Gorrie C, Schultz MB, Edwards DJ,
485 Nguyen KV, Nguyen TV, Dao TT, Mensink M, Minh VL, Nhu NTK, Schultsz C, Kuntaman
486 K, Newton PN, Moore CE, Strugnell RA, Thomson NR. 2015. Genomic analysis of
487 diversity, population structure, virulence, and antimicrobial resistance in Klebsiella
488 pneumoniae, an urgent threat to public health. PNAS 112:E3574–E3581.
489 13. Martin RM, Cao J, Wu W, Zhao L, Manthei DM, Pirani A, Snitkin E, Malani PN, Rao K,

490 Bachman MA. 2018. Identification of Pathogenicity-Associated Loci in Klebsiella
491 pneumoniae from Hospitalized Patients. mSystems 3.
492 14. Han JH, Lapp Z, Bushman F, Lautenbach E, Goldstein EJC, Mattei L, Hofstaedter CE, Kim
493 D, Nachamkin I, Garrigan C, Jain T, Bilker W, Wolford HM, Slayton RB, Wise J, Tolomeo
494 P, Snitkin ES. 2019. Whole-Genome Sequencing To Identify Drivers of Carbapenem-
495 Resistant Klebsiella pneumoniae Transmission within and between Regional Long-Term
496 Acute-Care Hospitals. Antimicrobial Agents and Chemotherapy 63.
497 15. Köster J, Rahmann S. 2012. Snakemake—a scalable bioinformatics workflow engine.
498 Bioinformatics 28:2520–2522.
499 16. Holt K. 2020. katholt/Kleborate. Python.
500 17. Wyres KL, Wick RR, Gorrie C, Jenney A, Follador R, Thomson NR, Holt KE. 2016.
501 Identification of Klebsiella capsule synthesis loci from whole genome data. Microbial
502 Genomics, 2:e000102.
503 18. Wick RR, Heinz E, Holt KE, Wyres KL. 2018. Kaptive Web: User-Friendly Capsule and
504 Lipopolysaccharide Serotype Prediction for Klebsiella Genomes. Journal of Clinical
505 Microbiology 56.
506 19. Lam MMC, Wick RR, Wyres KL, Gorrie CL, Judd LM, Jenney AWJ, Brisse S, Holt KE.
507 2018. Genetic diversity, mobilisation and spread of the yersiniabactin-encoding mobile
508 element ICEKp in Klebsiella pneumoniae populations. Microbial Genomics, 4:e000196.
509 20. Cingolani P, Platts A, Wang LL, Coon M, Nguyen T, Wang L, Land SJ, Lu X, Ruden DM.
510 2012. A program for annotating and predicting the effects of single nucleotide
511 polymorphisms, SnpEff. Fly 6:80–92.
512 21. Treepong P, Guyeux C, Meunier A, Couchoud C, Hocquet D, Valot B. 2018. panISa: ab
513 initio detection of insertion sequences in bacterial genomes from short read sequence
514 data. Bioinformatics 34:3795–3800.
515 22. Page AJ, Cummins CA, Hunt M, Wong VK, Reuter S, Holden MTG, Fookes M, Falush D,

516 Keane JA, Parkhill J. 2015. Roary: rapid large-scale prokaryote pan genome analysis.
517 Bioinformatics 31:3691–3693.
518 23. Li H, Handsaker B, Wysoker A, Fennell T, Ruan J, Homer N, Marth G, Abecasis G, Durbin
519 R. 2009. The Sequence Alignment/Map format and SAMtools. Bioinformatics 25:2078–
520 2079.
521 24. Croucher NJ, Page AJ, Connor TR, Delaney AJ, Keane JA, Bentley SD, Parkhill J, Harris
522 SR. 2015. Rapid phylogenetic analysis of large samples of recombinant bacterial whole
523 genome sequences using Gubbins. Nucleic Acids Res 43:e15–e15.
524 25. Nguyen L-T, Schmidt HA, von Haeseler A, Minh BQ. 2015. IQ-TREE: A Fast and Effective
525 Stochastic Algorithm for Estimating Maximum-Likelihood Phylogenies. Mol Biol Evol
526 32:268–274.
527 26. Minh BQ, Nguyen MAT, von Haeseler A. 2013. Ultrafast Approximation for Phylogenetic
528 Bootstrap. Mol Biol Evol 30:1188–1195.
529 27. 2020. 2020 NHSN Patient Safety Component Manual 434.
530 28. Saund K, Lapp Z, Thiede SN, Pirani A, Snitkin ES. 2020. prewas: data pre-processing for
531 more informative bacterial GWAS. Microbial Genomics, 6:e000368.
532 29. Topçuoğlu BD, Lesniak NA, Ruffin MT, Wiens J, Schloss PD. 2020. A Framework for
533 Effective Application of Machine Learning to Microbiome-Based Classification Problems.
534 mBio 11.
535 30. Kuhn M. 2008. Building Predictive Models in R Using the caret Package. 1. Journal of
536 Statistical Software 28:1–26.
537 31. R: The R Project for Statistical Computing.
538 32. Wickham H, Averick M, Bryan J, Chang W, McGowan L, François R, Grolemund G, Hayes
539 A, Henry L, Hester J, Kuhn M, Pedersen T, Miller E, Bache S, Müller K, Ooms J, Robinson
540 D, Seidel D, Spinu V, Takahashi K, Vaughan D, Wilke C, Woo K, Yutani H. 2019. Welcome
541 to the Tidyverse. Journal of Open Source Software 4:1686.

542 33. Wilke CO. 2019. cowplot: Streamlined Plot Theme and Plot Annotations for “ggplot2.”
543 34. Yu G, Smith DK, Zhu H, Guan Y, Lam TT-Y. 2017. ggtree: an r package for visualization
544 and annotation of phylogenetic trees with their covariates and other associated data.
545 Methods in Ecology and Evolution 8:28–36.
546 35. Yu G, Lam TT-Y, Zhu H, Guan Y. 2018. Two Methods for Mapping and Visualizing
547 Associated Data on Phylogeny Using Ggtree. Mol Biol Evol 35:3041–3043.
548 36. Paradis E, Schliep K. 2019. ape 5.0: an environment for modern phylogenetics and
549 evolutionary analyses in R. Bioinformatics 35:526–528.
550 37. grid package | R Documentation.
551 38. Popovich KJ, Snitkin ES, Hota B, Green SJ, Pirani A, Aroutcheva A, Weinstein RA. 2017.
552 Genomic and Epidemiological Evidence for Community Origins of Hospital-Onset
553 Methicillin-Resistant Staphylococcus aureus Bloodstream Infections. J Infect Dis
554 215:1640–1647.
555 39. Camacho C, Coulouris G, Avagyan V, Ma N, Papadopoulos J, Bealer K, Madden TL. 2009.
556 BLAST+: architecture and applications. BMC Bioinformatics 10:421.
557 40. Wattam AR, Davis JJ, Assaf R, Boisvert S, Brettin T, Bun C, Conrad N, Dietrich EM, Disz
558 T, Gabbard JL, Gerdes S, Henry CS, Kenyon RW, Machi D, Mao C, Nordberg EK, Olsen
559 GJ, Murphy-Olson DE, Olson R, Overbeek R, Parrello B, Pusch GD, Shukla M, Vonstein
560 V, Warren A, Xia F, Yoo H, Stevens RL. 2017. Improvements to PATRIC, the all-bacterial
561 Bioinformatics Database and Analysis Resource Center. Nucleic Acids Res 45:D535–
562 D542.
563 41. Li H, Durbin R. 2009. Fast and accurate short read alignment with Burrows–Wheeler
564 transform. Bioinformatics 25:1754–1760.
565 42. Follador R, Heinz E, Wyres KL, Ellington MJ, Kowarik M, Holt KE, Thomson NR. 2016. The
566 diversity of Klebsiella pneumoniae surface polysaccharides. Microb Genom 2.
567 43. Liu P, Li X, Luo M, Xu X, Su K, Chen S, Qing Y, Li Y, Qiu J. 2017. Risk Factors for

568 Carbapenem-Resistant Klebsiella pneumoniae Infection: A Meta-Analysis. Microbial Drug
569 Resistance 24:190–198.
570 44. Shankar-Sinha S, Valencia GA, Janes BK, Rosenberg JK, Whitfield C, Bender RA,
571 Standiford TJ, Younger JG. 2004. The Klebsiella pneumoniae O Antigen Contributes to
572 Bacteremia and Lethality during Murine Pneumonia. Infection and Immunity 72:1423–
573 1430.
574 45. Tedijanto C, Olesen SW, Grad YH, Lipsitch M. 2018. Estimating the proportion of
575 bystander selection for antibiotic resistance among potentially pathogenic bacterial flora.
576 Proceedings of the National Academy of Sciences 115:E11988–E11995.
577 46. Marsh JW, Mustapha MM, Griffith MP, Evans DR, Ezeonwuka C, Pasculle AW, Shutt KA,
578 Sundermann A, Ayres AM, Shields RK, Babiker A, Cooper VS, Tyne DV, Harrison LH.
579 2019. Evolution of Outbreak-Causing Carbapenem-Resistant Klebsiella pneumoniae
580 ST258 at a Tertiary Care Hospital over 8 Years. mBio 10:e01945-19.
581 47. Zhou K, Xiao T, David S, Wang Q, Zhou Y, Guo L, Aanensen D, Holt KE, Thomson NR,
582 Grundmann H, Shen P, Xiao Y. Novel Subclone of Carbapenem-Resistant Klebsiella
583 pneumoniae Sequence Type 11 with Enhanced Virulence and Transmissibility, China -
584 Volume 26, Number 2—February 2020 - Emerging Infectious Diseases journal - CDC
585 https://doi.org/10.3201/eid2602.190594.
586 48. Gu D, Dong N, Zheng Z, Lin D, Huang M, Wang L, Chan EW-C, Shu L, Yu J, Zhang R,
587 Chen S. 2018. A fatal outbreak of ST11 carbapenem-resistant hypervirulent Klebsiella
588 pneumoniae in a Chinese hospital: a molecular epidemiological study. The Lancet
589 Infectious Diseases 18:37–46.
590 49. Saund K, Snitkin ES. 2020. hogwash: Three Methods for Genome-Wide Association
591 Studies in Bacteria. bioRxiv 2020.04.19.048421.
592 50. Chapman SJ, Hill AVS. 2012. Human genetic susceptibility to infectious disease. 3. Nat
593 Rev Genet 13:175–188.

Main figures

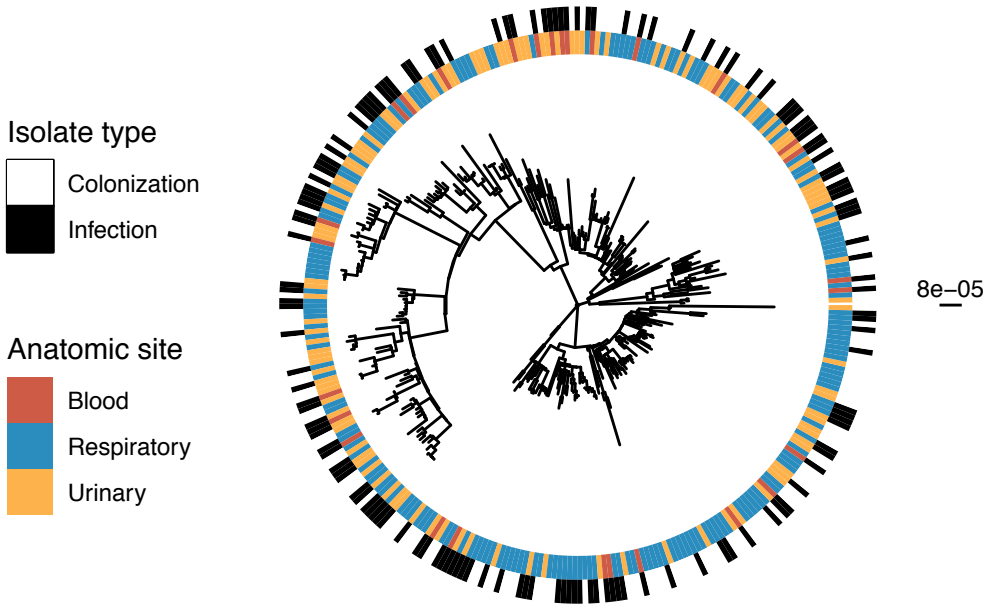

Figure 1: Infection and anatomic site cluster on the phylogeny. Maximum likelihood phylogenetic tree of all isolates including infection or colonization classification for each isolate and anatomic site of isolation. The scale bar to the right of the phylogeny shows the branch length in substitutions per site. Testing for non-random distribution of isolates on the phylogeny (see supplementary methods) revealed clustering of infection, respiratory, and urinary isolates on the phylogeny, respectively.

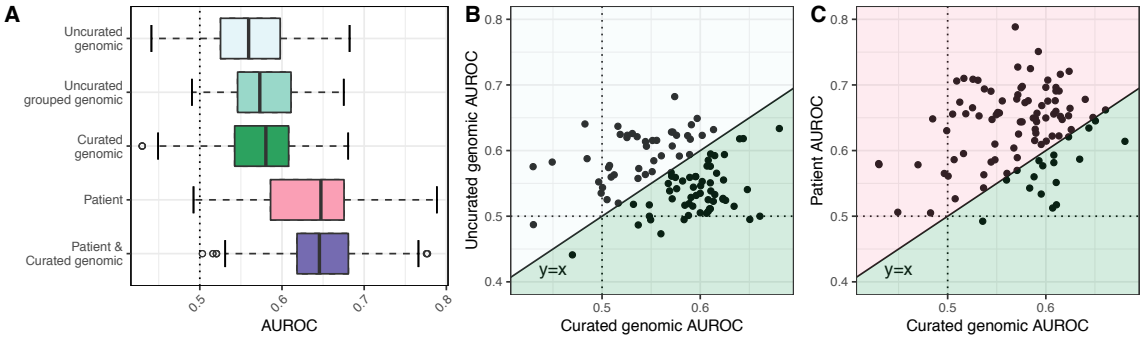

Figure 2: Test AUROCs for various classifiers identifying CRKP colonization vs. infection vary substantially across data splits. (A) Test AUROCs for 100 L2 regularized logistic regression models different using train/test splits. All isolates from a given LTACH were included in either the training split or the testing split for each data split. We built models using five different feature sets, keeping the same

607 100 data splits. AUROCs of different feature sets were not significantly different. In the right two panels,
608 the curated genomic feature set AUROCs are compared to: (B) the uncurated genomic feature set
609 AUROCs, and (C) the patient feature set AUROCs. Each point is the resulting pair of AUROCs for models
610 built with the same data split, but the two respective feature sets. The dotted lines in all 3 panels indicate
611 the AUROC for choosing an outcome randomly (0.5); anything below the line is worse than random, and
612 anything above the line is better than random. The solid diagonal line in the right two panels is the line
613 y=x; points below the line correspond to a higher curated genomic AUROC for that data split, and points
614 above the line correspond to a higher uncurated genomic AUROC (B), or patient AUROC (C),
615 respectively. The colors in panels (B) and (C) correspond to the colors in panel (A); the points in a given
616 colored area indicate that that feature set had the higher AUROC for that data split. In both cases, one
617 feature set does not consistently outperform the other (p=0.4; see supplementary methods for p-value
618 calculation). AUROC=area under the receiver operating characteristic curve.

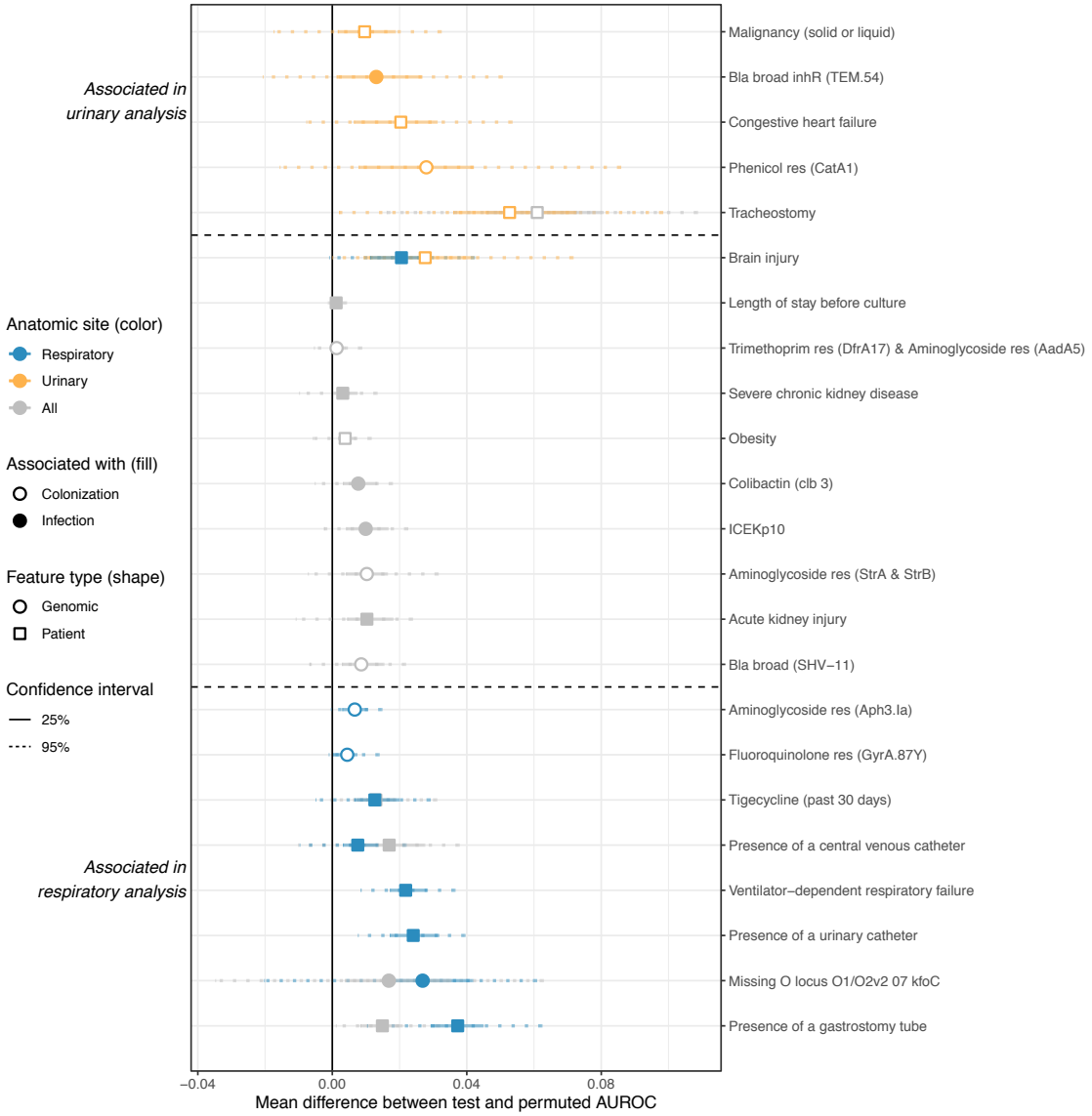

Figure 3: Features consistently associated with colonization or infection sometimes differ between the overall, respiratory, and urinary models. Feature-specific improvement in model performance, measured as the mean difference between test and permuted AUROC (see methods), of features found to be consistently associated with colonization or infection in at least one of the following analyses: overall, respiratory-specific, urinary-specific. We consider features to be associated with infection/colonization if the AUROC difference was greater than zero in over 75% of the 100 data splits. The vertical solid black line indicates a difference of zero (i.e. the feature provides no improvement to model performance). Horizontal dotted lines separate features associated with urinary but not respiratory isolates (top), both urinary and respiratory (or all) isolates (middle), or respiratory but not urinary isolates

629 (bottom). Bla=Beta lactamase, res=confers resistance to that antibiotic class. AUROC=area under the

630 receiver operating characteristic curve.

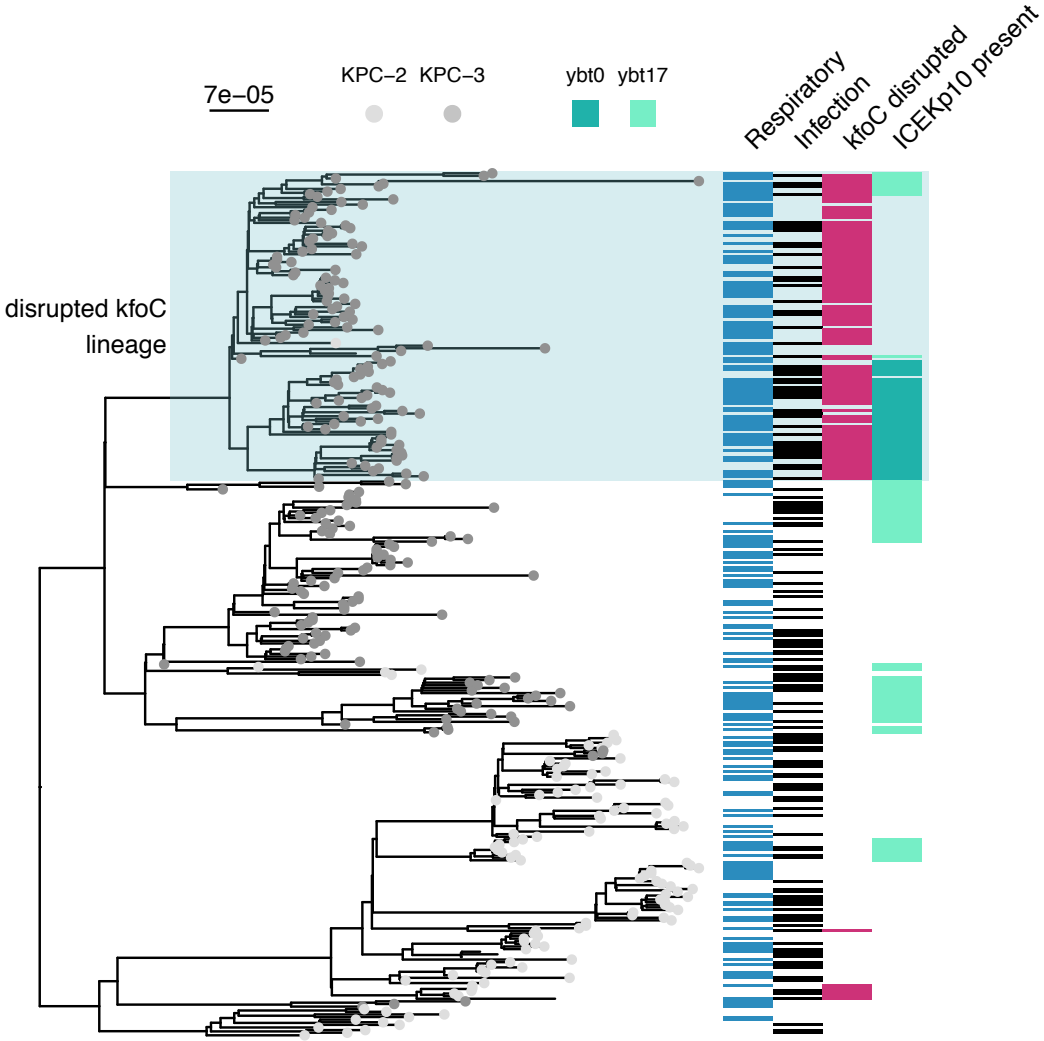

631

632 **Figure 4: Select epidemiologic and genomic features visualized on the phylogeny indicate that a**

633 **sub-clade of ST258 clade II may exhibit enhanced niche-specific adaptation and virulence.** ST258

634 maximum likelihood phylogeny with the tip labels colored by KPC gene. The blue box indicates the sub-

635 lineage with apparent altered niche-specific adaptation that acquires an additional virulence locus. The

636 heatmap beside the tree indicates information about the isolate. From left to right: if it is a respiratory

637 isolate, if it is an infection isolate, if *kfoC* is disrupted, and if it contains ICEKp10. Disrupted *kfoC* was

638 associated with infection in the overall and respiratory machine learning analyses and ICEKp10 presence

639 was associated with infection in the overall analysis. The scale bar to the top left of the phylogeny shows
640 the branch length in substitutions per site. ybt=Yersiniabactin; ybt0 and ybt17 are two ybtSTs defined by
641 Kleborate.
642

643 ## Supplementary materials

644

645 ### Supplementary methods

646

647 #### Pipeline

648 We created a snakemake pipeline (1) to perform data pre-processing, machine learning analysis, and
649 figure generation.
650

651 #### Genomic data

652 We used Kleborate version 0.3.0 (2) to identify sequence type, capsular types (K locus (3) and O locus
653 (4)), virulence factor (5), and antibiotic resistance genes. In addition, we identified single nucleotide
654 variants (SNVs) and indels by mapping reads to the KPNIH1 reference genome (BioProject accession
655 number PRJNA73191; https://github.com/Snitkin-Lab-Umich/variant_calling_pipeline (6)). After variant
656 calling, we identified the predicted functional impact of variants using SnpEff version 4.3T (7). We also
657 identified large insertion sequence (IS) elements using panISa version 0.1.4 with the default settings (8),
658 and accessory genome genes using Roary version 3.12.0 with the default settings (9).
659

660 #### Phylogenetic tree reconstruction

661 We constructed a phylogenetic tree of all ST258 isolates by first creating a whole-genome alignment by
662 mapping reads to the KPNIH1 reference genome (GenBank accession number CP008827.1) using bwa
663 mem version 0.7.12 (10); samtools version 1.9 (11) was used to generate binary alignment files. We then
664 masked sites identified as recombinant by Gubbins version 2.3.2 (12) and used this masked whole-

genome alignment to build a maximum likelihood phylogeny with IQ-TREE version 1.6.12 (13) using a GTR model of nucleotide substitution and ultra-fast bootstrap with 1000 replicates (-b 1000) (14). The tree was midpoint-rooted using the midpoint.root function in phytools version 0.6-99 (15), thus splitting the tree into ST258 clades I and II (16).

Phylogenetic clustering test

To determine whether infection isolates cluster on the phylogeny more than expected by random chance, we performed a permutation test (17). To identify the true number of isolates in a pure cluster while controlling for isolate clustering by LTACH, we enumerated isolates in pure infection or colonization subtrees that also contain isolates from more than one LTACH. Then we randomized the infection labels across isolates 1000 times and enumerated the number of isolates in a pure subtree for each randomization. We then compared the random counts of isolates in a pure cluster to the true number and calculated an empirical p-value.

Feature set pre-processing

We used five feature sets to study the association between infection and colonization. To determine how well machine learning models perform using a targeted vs. untargeted approach, we performed machine learning with uncurated genomic features as well as curated genomic features known to be related to virulence. In an attempt to increase power, we not only performed machine learning on individual uncurated genomic features, but also using a burden test where genomic variants were grouped into genes and features were presence/absence of a variant in a gene. This may help capture variation associated with infection at the gene level that might not be captured at the variant level (e.g. different samples can have different variants in the same gene that all lead to a similar function). For the uncurated grouped genomic analysis, grouped variants included SNVs and indels identified as moderate or high impact by SnpEff and IS elements in a gene or upstream of a gene. We also grouped modifier variants identified by SnpEff into intergenic regions. Only features that occurred in more than one isolate and less than n-1 isolates were included. For the uncurated genomic and uncurated grouped genomic datasets we

692 collapsed genomic features with an identical pattern across all isolates to reduce machine learning
693 runtime.
694
695 **Machine learning rationale**
696 We chose to perform L2 regularized logistic regression because it is easily interpretable, often performs
697 just as well as more complicated methods when limited training data are available (18), and has a
698 grouping effect, which means that all associated features are identified even if they are collinear (19).
699
700 **Machine learning details**
701 The machine learning pipeline removes variables with near-zero variance, normalizes all features to be
702 between zero and one, and sets at least 20% of the data aside for testing in each train/test split. We split
703 the training data into train and validate sets by LTACH using the groupKMultiFolds function from the caret
704 R package (caret version 6.0-85) (20). Within each training set, we selected hyperparameters via five-fold
705 cross-validation 100 times, maximizing the average cross-validation AUROC.
706
707 **Comparing model performance between feature sets**
708 To determine whether there was a significant difference in model performance between different feature
709 sets, we calculated a two-sided empirical p-value for each identical train/test split using the formula (2 x
710 min(fraction of AUROC differences ≥ 0, fraction of AUROC differences ≤ 0) (18).
711
712 **Identification of IS element insertions in certain O2v2 kfoC genes**
713 One of the curated genomic features we identified as associated with infection was what Kleborate called
714 a missing gene (kfoC) in the O locus operon of certain O2v2 serotypes. On the Kleborate website, they
715 indicate that a missing gene could represent a truly missing gene, or a gene that is split between two
716 different contigs. To further investigate this, we used blastn version 2.9.0 (21) to search for kfoC genes in
717 each of the samples. Additionally, we aligned the reads of all genomes to CP031810, a complete *K.*

718 *pneumoniae* genome from PATRIC (22) using bwa mem version 0.7.12 (10), and samtools (11) was used
719 to generate binary alignment files. Next, we used panISa (8) to identify IS element insertions in kfoC.
720
721 **Data analysis & visualization**
722 We used Fisher's exact tests for bivariable analyses with categorical variables, and Wilcoxon rank-sum
723 tests for bivariable analyses with continuous variables. We performed all data analysis and visualization
724 in R version 3.6.2 (23) using the following packages: tidyverse version 1.3.0 (24), cowplot version 1.0.0
725 (25), ggtree version 2.0.1 (26, 27), ape version 5.3 (28), phytools version 0.6-99 (15), and grid version
726 3.6.2 (29).
727
728 **Supplementary results**
729
730 **Patients with different sequence types show no substantive differences in infection status,**
731 **anatomic site of isolation, or clinical characteristics**
732 Over 90% of the isolates in our dataset were ST258 (**Table S2**), the dominant strain in the US (30). At the
733 level of sequence type, we found no difference in infection prevalence (p=0.44) or anatomic site of
734 isolation (p=0.66), indicating that at this coarse level there was not evidence of differences in strain
735 virulence or adaptation to a certain anatomic site. Bivariable comparison of patient factors between
736 patients with different sequence types revealed only four significant differences (unadjusted p-values <
737 0.05; previous use of piperacillin/tazobactam, cefepime, ciprofloxacin, or fluoroquinolones). As we found
738 no substantive differences in infection, anatomic site of isolation, or patient variables when comparing
739 different sequence types, we chose to focus all subsequent analyses on ST258, the dominant sequence
740 type in our dataset. The genetic variation of isolates within ST258 is much smaller than the genetic
741 variation between sequence types, so limiting our analyses to ST258 could improve our ability to identify
742 associations of interest within ST258.
743
744 **Supplementary references**

1. Köster J, Rahmann S. 2012. Snakemake—a scalable bioinformatics workflow engine. Bioinformatics 28:2520–2522.

2. Holt K. 2020. katholt/Kleborate. Python.

3. Wyres KL, Wick RR, Gorrie C, Jenney A, Follador R, Thomson NR, Holt KE. 2016. Identification of Klebsiella capsule synthesis loci from whole genome data. Microbial Genomics, 2:e000102.

4. Wick RR, Heinz E, Holt KE, Wyres KL. 2018. Kaptive Web: User-Friendly Capsule and Lipopolysaccharide Serotype Prediction for Klebsiella Genomes. Journal of Clinical Microbiology 56.

5. Lam MMC, Wick RR, Wyres KL, Gorrie CL, Judd LM, Jenney AWJ, Brisse S, Holt KE. 2018. Genetic diversity, mobilisation and spread of the yersiniabactin-encoding mobile element ICEKp in Klebsiella pneumoniae populations. Microbial Genomics, 4:e000196.

6. Conlan S, Park M, Deming C, Thomas PJ, Young AC, Coleman H, Sison C, Program NCS, Weingarten RA, Lau AF, Dekker JP, Palmore TN, Frank KM, Segre JA. 2016. Plasmid Dynamics in KPC-Positive Klebsiella pneumoniae during Long-Term Patient Colonization. mBio

7. Cingolani P, Platts A, Wang LL, Coon M, Nguyen T, Wang L, Land SJ, Lu X, Ruden DM. 2012. A program for annotating and predicting the effects of single nucleotide polymorphisms, SnpEff. Fly (Austin) 6:80–92.

8. Treepong P, Guyeux C, Meunier A, Couchoud C, Hocquet D, Valot B. 2018. panISa: ab initio detection of insertion sequences in bacterial genomes from short read sequence data. Bioinformatics 34:3795–3800.

9. Page AJ, Cummins CA, Hunt M, Wong VK, Reuter S, Holden MTG, Fookes M, Falush D, Keane JA, Parkhill J. 2015. Roary: rapid large-scale prokaryote pan genome analysis. Bioinformatics 31:3691–3693.

10. Li H, Durbin R. 2009. Fast and accurate short read alignment with Burrows–Wheeler transform. Bioinformatics 25:1754–1760.

771 11. Li H, Handsaker B, Wysoker A, Fennell T, Ruan J, Homer N, Marth G, Abecasis G, Durbin R.
772 2009. The Sequence Alignment/Map format and SAMtools. Bioinformatics 25:2078–2079.
773 12. Croucher NJ, Page AJ, Connor TR, Delaney AJ, Keane JA, Bentley SD, Parkhill J, Harris SR.
774 2015. Rapid phylogenetic analysis of large samples of recombinant bacterial whole genome
775 sequences using Gubbins. Nucleic Acids Res 43:e15–e15.
776 13. Nguyen L-T, Schmidt HA, von Haeseler A, Minh BQ. 2015. IQ-TREE: A Fast and Effective
777 Stochastic Algorithm for Estimating Maximum-Likelihood Phylogenies. Mol Biol Evol 32:268–274.
778 14. Minh BQ, Nguyen MAT, von Haeseler A. 2013. Ultrafast Approximation for Phylogenetic
779 Bootstrap. Mol Biol Evol 30:1188–1195.
780 15. Revell LJ. 2012. phytools: an R package for phylogenetic comparative biology (and other
781 things). Methods in Ecology and Evolution 3:217–223.
782 16. DeLeo FR, Chen L, Porcella SF, Martens CA, Kobayashi SD, Porter AR, Chavda KD, Jacobs
783 MR, Mathema B, Olsen RJ, Bonomo RA, Musser JM, Kreiswirth BN. 2014. Molecular dissection of
784 the evolution of carbapenem-resistant multilocus sequence type 258 Klebsiella pneumoniae. PNAS
785 111:4988–4993.
786 17. Popovich KJ, Snitkin ES, Hota B, Green SJ, Pirani A, Aroutcheva A, Weinstein RA. 2017.
787 Genomic and Epidemiological Evidence for Community Origins of Hospital-Onset Methicillin-
788 Resistant Staphylococcus aureus Bloodstream Infections. J Infect Dis 215:1640–1647.
789 18. Topçuoğlu BD, Lesniak NA, Ruffin M, Wiens J, Schloss PD. 2019. Effective application of
790 machine learning to microbiome-based classification problems. bioRxiv 816090.
791 19. Schreiber-Gregory DN, Waller J, Smith T. 2018. Ridge Regression and multicollinearity: An in-
792 depth review. Model Assisted Statistics & Applications 13:359–365.
793 20. Kuhn M. 2008. Building Predictive Models in R Using the caret Package. 1. Journal of
794 Statistical Software 28:1–26.
795 21. Camacho C, Coulouris G, Avagyan V, Ma N, Papadopoulos J, Bealer K, Madden TL. 2009.
796 BLAST+: architecture and applications. BMC Bioinformatics 10:421.

797 22. Wattam AR, Davis JJ, Assaf R, Boisvert S, Brettin T, Bun C, Conrad N, Dietrich EM, Disz T,
798 Gabbard JL, Gerdes S, Henry CS, Kenyon RW, Machi D, Mao C, Nordberg EK, Olsen GJ, Murphy-
799 Olson DE, Olson R, Overbeek R, Parrello B, Pusch GD, Shukla M, Vonstein V, Warren A, Xia F, Yoo
800 H, Stevens RL. 2017. Improvements to PATRIC, the all-bacterial Bioinformatics Database and
801 Analysis Resource Center. Nucleic Acids Res 45:D535–D542.
802 23. R: The R Project for Statistical Computing.
803 24. Wickham H, Averick M, Bryan J, Chang W, McGowan L, François R, Grolemund G, Hayes A,
804 Henry L, Hester J, Kuhn M, Pedersen T, Miller E, Bache S, Müller K, Ooms J, Robinson D, Seidel D,
805 Spinu V, Takahashi K, Vaughan D, Wilke C, Woo K, Yutani H. 2019. Welcome to the Tidyverse.
806 Journal of Open Source Software 4:1686.
807 25. Wilke CO. 2019. cowplot: Streamlined Plot Theme and Plot Annotations for “ggplot2.”
808 26. Yu G, Smith DK, Zhu H, Guan Y, Lam TT-Y. 2017. ggtree: an r package for visualization and
809 annotation of phylogenetic trees with their covariates and other associated data. Methods in Ecology
810 and Evolution 8:28–36.
811 27. Yu G, Lam TT-Y, Zhu H, Guan Y. 2018. Two Methods for Mapping and Visualizing Associated
812 Data on Phylogeny Using Ggtree. Mol Biol Evol 35:3041–3043.
813 28. Paradis E, Schliep K. 2019. ape 5.0: an environment for modern phylogenetics and
814 evolutionary analyses in R. Bioinformatics 35:526–528.
815 29. grid package | R Documentation.
816 30. Wyres KL, Lam MMC, Holt KE. 2020. Population genomics of Klebsiella pneumoniae. Nature
817 Reviews Microbiology 1–16.
818

819 **Supplementary tables & figures**

820 **Table S1: Infection status and anatomic site of isolation by CRKP sequence type.**

Sequence Type	Colonization		Infection			Total (%)
	Respiratory	Urinary	Blood	Respiratory	Urinary	
ST15	4	3	1	2	0	10 (2.8)
ST15-1LV	0	0	0	1	0	1 (0.3)
ST17	0	0	0	2	0	2 (0.6)
ST2237	0	1	0	0	0	1 (0.3)
ST258	121	71	28	62	49	331 (93.2)
ST307	1	4	0	2	2	9 (2.5)
ST36	1	0	0	0	0	1 (0.3)

821

822 **Table S2: Definitions of infection for urinary and respiratory cultures.**

Source	Infection definition
Urinary	≥100,000 colony-forming units/mL on urinary culture with no more than 2 species of microorganisms AND at least one of the following: ● Leukocytosis (≥10,000 cells/μL) ≤ 7 days prior to specimen collection ● Positive urinalysis demonstrated by at least one of the following findings: ○ Positive dipstick for leukocyte esterase and/or nitrate ○ Pyuria (urinary specimen with ≥ 10 white blood cells/mL or ≥ 3 white blood cells/high power field of unspun urinary) ○ Microorganisms seen on Gram stain of unspun urinary

Respiratory	Chest X-ray with interpretation of pneumonia, probable pneumonia, or infiltrate/consolidation AND leukocytosis (≥10,000 cells/μL) ≤ 7 days prior to specimen collection

823

824 **Table S3: Bivariable analysis of patient features associated with CRKP ST258 infection in LTACH**

825 **residents.**

Variable	Infection (n=139)	Colonization (n=192)	All		Respiratory		Urinary	
			OR (95% CI)	P value	OR (95% CI)	P value	OR (95% CI)	P value
Blood culture	28 (20%)	0 (0%)	-	-	-	-	-	-
Respiratory culture	62 (45%)	121 (63%)	0.47 (0.3-0.76)	0.0011	-	-	-	-
Urinary culture	49 (35%)	71 (37%)	0.93 (0.57-1.5)	0.82	-	-	-	-
Admission to an LTACH in the year prior to culture[1]	9 (6%)	7 (4%)	1.83 (0.59-5.93)	0.30	2.03 (0.45-9.19)	0.31	2.23 (0.25-27.73)	0.40
Length of stay before culture, median (IQR)[2]	23 (9.0-50)	18 (2.0-34)	-	0.98	-	0.66	-	0.88
Age, median (IQR)[2]	72 (64-79)	73 (64-83)	-	0.029	-	0.0010	-	0.55
Sex (male)	74 (53%)	102 (53%)	1 (0.63-1.59)	1.0	1.15 (0.59-2.29)	0.75	0.94 (0.42-2.1)	1.0

Presence of a central venous catheter	87 (63%)	97 (51%)	1.64 (1.03-2.62)	0.033	3.36 (1.54-7.87)	0.00094	0.79 (0.34-1.81)	0.57
Tracheostomy	83 (60%)	141 (73%)	0.54 (0.33-0.88)	0.0091	1.45 (0.41-6.51)	0.78	0.42 (0.17-0.99)	0.035
Presence of a urinary catheter	87 (63%)	94 (49%)	1.74 (1.09-2.79)	0.019	4.19 (2.06-8.88)	0.000020	0.71 (0.32-1.59)	0.45
Congestive heart failure	27 (19%)	38 (20%)	0.98 (0.54-1.75)	1.0	1.74 (0.8-3.76)	0.14	0.25 (0.04-0.95)	0.035
Acute or chronic respiratory failure	55 (40%)	66 (34%)	1.25 (0.77-2.01)	0.36	1.93 (0.99-3.78)	0.040	0.68 (0.27-1.64)	0.42
Acute kidney injury	76 (55%)	76 (40%)	1.84 (1.16-2.93)	0.0074	2.65 (1.36-5.29)	0.0028	1.18 (0.53-2.62)	0.71
Malignancy (solid or liquid)	16 (12%)	27 (14%)	0.8 (0.38-1.61)	0.51	0.97 (0.31-2.76)	1.0	0.62 (0.18-1.94)	0.45
Brain injury[3]	31 (22%)	31 (16%)	1.49 (0.82-2.7)	0.20	3.37 (1.57-7.32)	0.00082	0.1 (0-0.75)	0.014
Presence of a gastrostomy tube	62 (45%)	59 (31%)	1.81 (1.12-2.93)	0.011	2.98 (1.52-5.94)	0.00083	1.45 (0.61-3.44)	0.42
Obesity[4]	4 (3%)	14 (7%)	0.38 (0.09-1.24)	0.091	0.23 (0.01-1.81)	0.28	0.46 (0.04-2.74)	0.47
Malnourished/underweight[5]	38 (27%)	43 (22%)	1.3 (0.76-	0.30	2.02 (0.94-4.32)	0.065	0.66 (0.24-1.67)	0.39

			2.22)					
Transplant[6]	4 (3%)	3 (2%)	1.86 (0.31-12.93)	0.46	3.01 (0.33-36.91)	0.34	1.45 (0.02-115.98)	1.0
Cirrhosis	8 (6%)	6 (3%)	1.89 (0.56-6.77)	0.28	3.43 (0.64-22.82)	0.12	0.47 (0.01-6.12)	0.64
Severe chronic kidney disease[7]	52 (37%)	55 (29%)	1.49 (0.91-2.43)	0.097	2.12 (1.08-4.19)	0.023	1.06 (0.42-2.63)	1.0
Pulmonary disease[8]	25 (18%)	34 (18%)	1.02 (0.55-1.87)	1.0	1.09 (0.44-2.6)	0.84	0.68 (0.21-1.99)	0.48
Ventilator-dependent respiratory failure	52 (37%)	48 (25%)	1.79 (1.09-2.96)	0.021	3.34 (1.69-6.69)	0.00023	0.49 (0.11-1.78)	0.27
Stage IV/V decubitus ulcer	31 (22%)	32 (17%)	1.43 (0.79-2.58)	0.20	2.02 (0.94-4.32)	0.065	1.54 (0.5-4.81)	0.44
Amikacin[9]	23 (17%)	14 (7%)	2.51 (1.18-5.52)	0.013	1.88 (0.63-5.49)	0.21	2.77 (0.66-13.69)	0.12
Aztreonam[9]	5 (4%)	6 (3%)	1.16 (0.27-4.65)	1.0	1.99 (0.26-15.34)	0.41	0 (0-3.49)	0.27
Trimethoprim/sulfamethoxazole[9]	6 (4%)	5 (3%)	1.68 (0.42-7.13)	0.54	1.99 (0.26-15.34)	0.41	1.46 (0.1-20.84)	1.0
Cefepime[9]	20 (14%)	32 (17%)	0.84 (0.43-1.6)	0.65	1.1 (0.42-2.73)	0.83	0.57 (0.17-1.74)	0.33

Ceftaroline[9]	4 (3%)	3 (2%)	1.86 (0.31-12.93)	0.46	0 (0-4.73)	0.55	Inf (0.61-Inf)	0.066
Ceftazidime[9]	3 (2%)	7 (4%)	0.58 (0.1-2.61)	0.53	0.97 (0.15-4.76)	1.0	0 (0-56.46)	1.0
Ceftriaxone[9]	11 (8%)	8 (4%)	1.97 (0.7-5.82)	0.16	1.68 (0.39-6.91)	0.51	3.04 (0.42-34.89)	0.22
Ciprofloxacin[9]	2 (1%)	6 (3%)	0.45 (0.04-2.59)	0.48	1.96 (0.02-155.49)	1.0	0 (0-1.55)	0.078
Colistin[9]	12 (9%)	11 (6%)	1.55 (0.61-4.02)	0.38	2.4 (0.72-8.22)	0.15	0.35 (0.01-3.7)	0.65
Daptomycin[9]	10 (7%)	3 (2%)	4.86 (1.22-28)	0.018	8.18 (0.79-409.93)	0.046	4.75 (0.8-50.2)	0.062
Ertapenem[9]	6 (4%)	4 (2%)	2.12 (0.49-10.4)	0.33	3.97 (0.2-237.55)	0.27	0.47 (0.01-6.12)	0.64
Metronidazole[9]	25 (18%)	35 (18%)	0.98 (0.53-1.8)	1.0	0.97 (0.43-2.11)	1.0	1.27 (0.33-4.77)	0.77
Gentamicin[9]	5 (4%)	5 (3%)	1.39 (0.31-6.19)	0.75	0.98 (0.09-7.03)	1.0	2.95 (0.15-178)	0.57
Imipenem[9]	3 (2%)	2 (1%)	2.09 (0.24-25.36)	0.65	1.96 (0.02-155.49)	1.0	0 (0-56.46)	1.0
Levofloxacin[9]	18 (13%)	25 (13%)	0.99 (0.49-1.99)	1.0	1.57 (0.63-3.85)	0.29	0.61 (0.13-2.37)	0.56

Linezolid[9]	23 (17%)	22 (11%)	1.53 (0.77-3.03)	0.20	1.47 (0.54-3.83)	0.49	1.1 (0.29-3.91)	1.0
Meropenem[9]	39 (28%)	50 (26%)	1.11 (0.66-1.86)	0.71	1.13 (0.54-2.31)	0.73	0.88 (0.32-2.33)	0.83
Polymyxin[9]	8 (6%)	4 (2%)	2.86 (0.75-13.26)	0.13	0.98 (0.09-7.03)	1.0	Inf (0.27-Inf)	0.16
Tigecycline[9]	25 (18%)	17 (9%)	2.25 (1.11-4.66)	0.019	2.63 (1.04-6.75)	0.026	2.55 (0.68-10.63)	0.14
Tobramycin[9]	7 (5%)	10 (5%)	0.97 (0.3-2.89)	1.0	0.47 (0.05-2.47)	0.50	2.23 (0.25-27.73)	0.40
Piperacillin/tazobactam[9]	18 (13%)	23 (12%)	1.09 (0.53-2.22)	0.87	0.9 (0.29-2.52)	1.0	1.53 (0.46-5.09)	0.43
Intravenous vancomycin[9]	52 (37%)	62 (32%)	1.25 (0.77-2.03)	0.35	1.07 (0.54-2.09)	0.87	1.03 (0.4-2.6)	1.0
Aminoglycoside[9]	32 (23%)	27 (14%)	1.82 (1-3.36)	0.042	1.14 (0.47-2.66)	0.84	2.75 (0.83-9.98)	0.099
Polymyxin or colistin[9]	20 (14%)	15 (8%)	1.98 (0.92-4.34)	0.070	1.92 (0.68-5.33)	0.22	1.09 (0.15-6.78)	1.0
Third-generation cephalosporin[9]	14 (10%)	15 (8%)	1.32 (0.57-3.05)	0.56	1.34 (0.45-3.82)	0.62	2 (0.32-14.33)	0.44
Anti-pseudomonal antibiotic[9,10]	88 (63%)	115 (60%)	1.15 (0.72-1.86)	0.57	1.24 (0.63-2.49)	0.52	0.76 (0.34-1.69)	0.58

Fluoroquinolone[9]	20 (14%)	31 (16%)	0.87 (0.45-1.67)	0.76	1.62 (0.67-3.86)	0.29	0.36 (0.08-1.27)	0.12
Carbapenem[9]	59 (42%)	68 (35%)	1.34 (0.84-2.16)	0.21	1.26 (0.64-2.45)	0.52	0.98 (0.41-2.31)	1.0
Piperacillin/tazobactam or ceftazidime[9]	20 (14%)	29 (15%)	0.94 (0.48-1.82)	0.88	0.86 (0.32-2.14)	0.83	1.34 (0.41-4.28)	0.60

[1]LTACH=long-term acute care hospital
[2]IQR=interquartile range
[3]Anoxic brain injury or cerebrovascular accident (CVA) causing paresis
[4]BMI ≥30 kg/m^2
[5]BMI ≤18.5 kg/m^2
[6]Solid organ transplant or hematopoeitic stem cell transplant
[7]Stage IV or dialysis
[8]Chronic obstructive pulmonary disease (COPD) or chronic bronchitis
[9]Receipt for ≥48 hours in the 30 days prior to culture
[10]Aminoglycosides, cefepime, ceftazidime, fluoroquinolones, polymyxins, carbapenems, or piperacillin-tazobactam

826

827

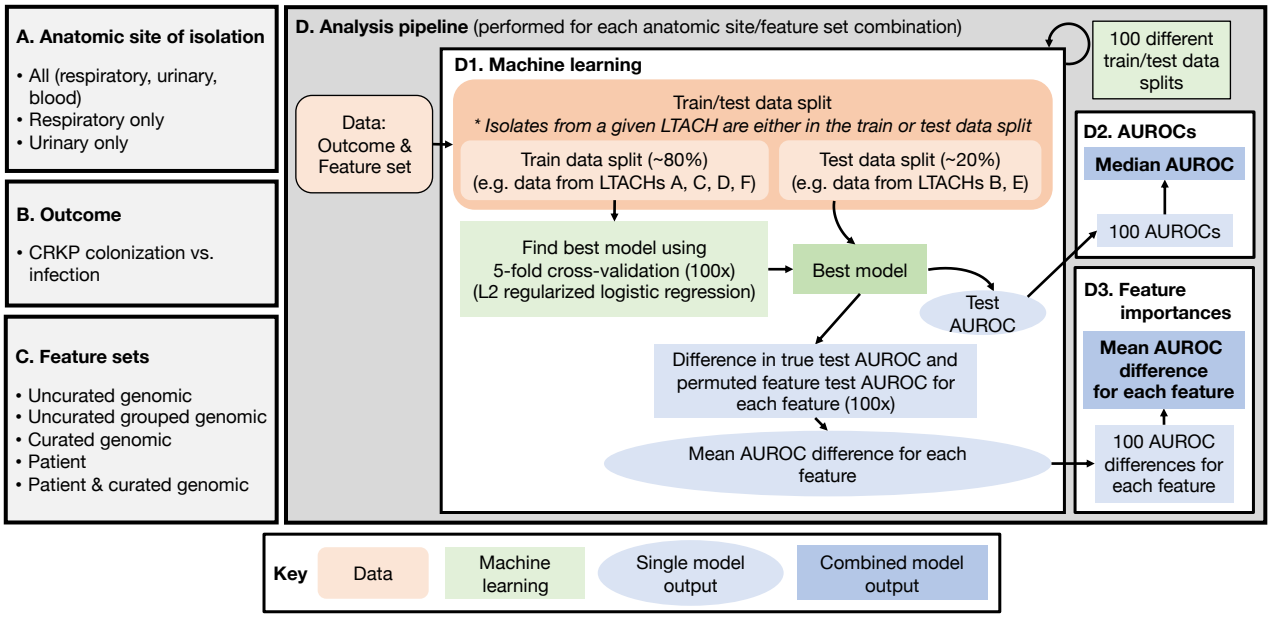

Figure S1: Methods overview. (A) Isolate subsets, based on anatomic site, used for different machine learning analyses. (B) Outcome used for all machine learning analyses. (C) Feature sets used for machine learning analyses (see main methods for more details). (D) Machine learning analysis pipeline: (D1) Machine learning pipeline, (D2) Median AUROC calculated from machine learning pipeline, (D3) Mean difference in test vs. permuted AUROC for each feature (see methods for more details). AUROC=area under the receiver operating characteristic curve.

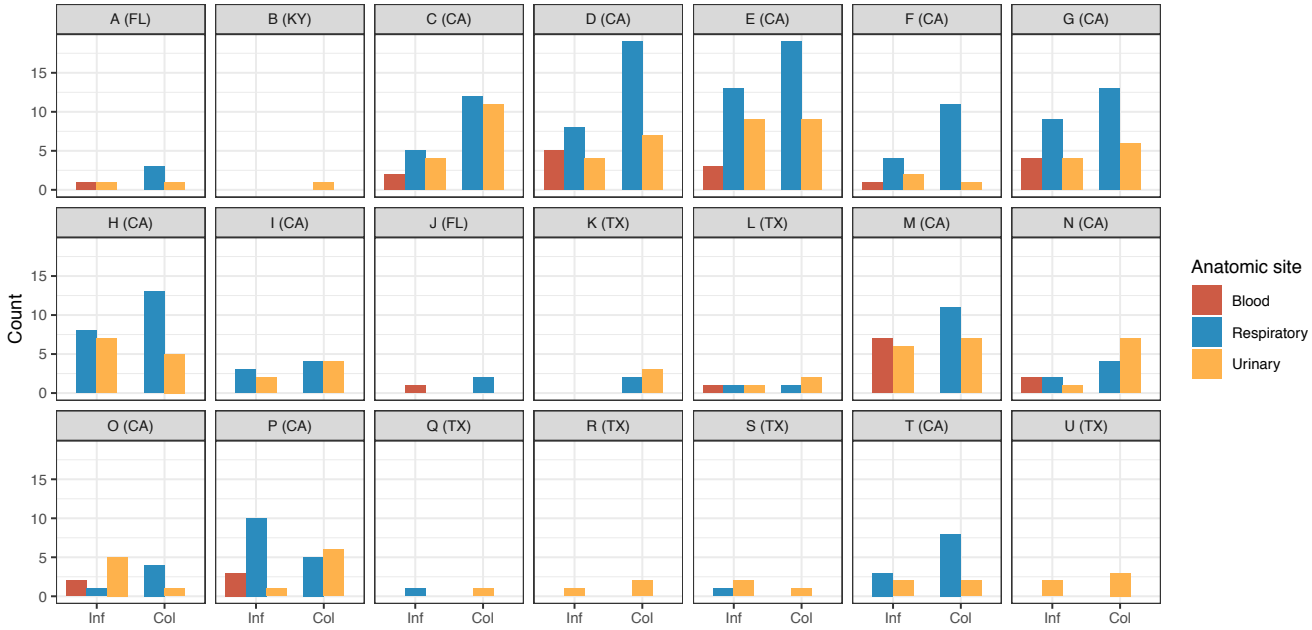

Figure S2: There are differences in sample size and distribution of infection and anatomic site of samples across LTACHs. Distribution of colonization and infection isolates are split by source and LTACH of origin. A to U are specific LTACHs and the geographic location by state is in parentheses. LTACH=long-term acute care hospital.

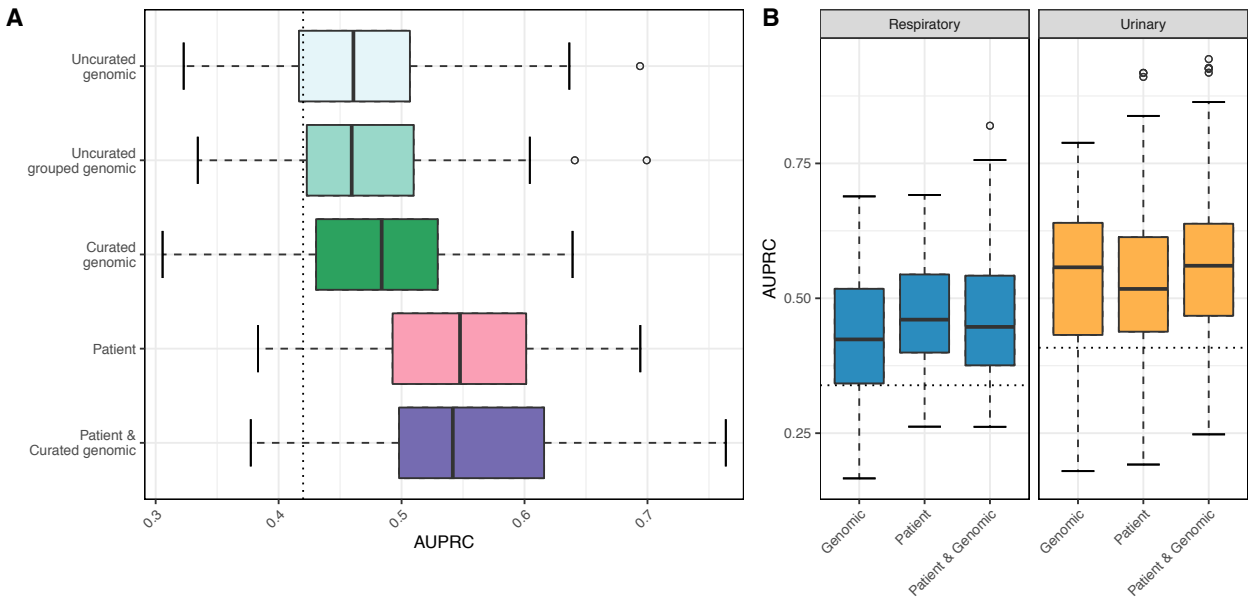

Figure S3: Test AUPRCs for various classifiers identifying CRKP colonization vs. infection for the overall machine learning model and respiratory and urinary models. Test AUPRCs for 100 train/test splits used to build classifiers with L2 regularized logistic regression. (A) Overall model with various classifiers. (B) Respiratory and urinary models; the curated genomic feature set was used here. AUPRC=area under the precision recall curve.

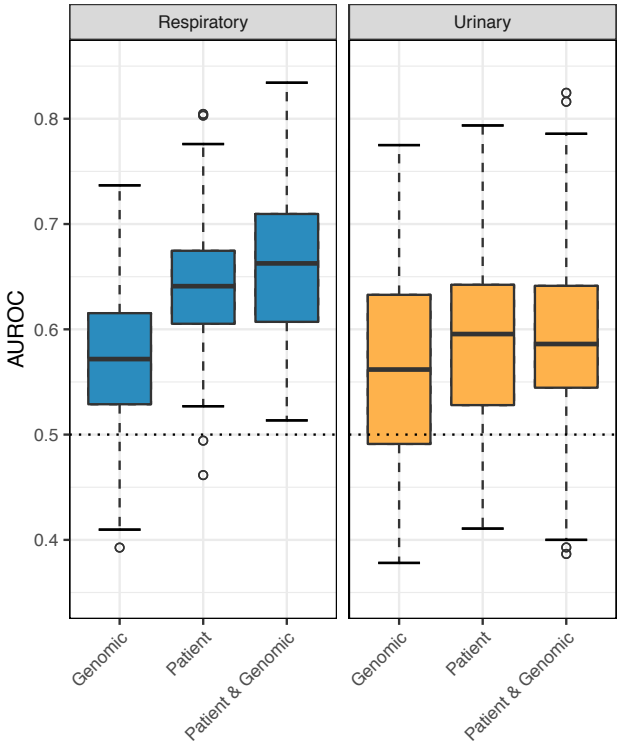

Figure S4: Test AUROC of respiratory and urinary ST258 only machine learning models for various feature sets. The curated genomic feature set was used here. AUROC=area under the receiver operating characteristic curve.

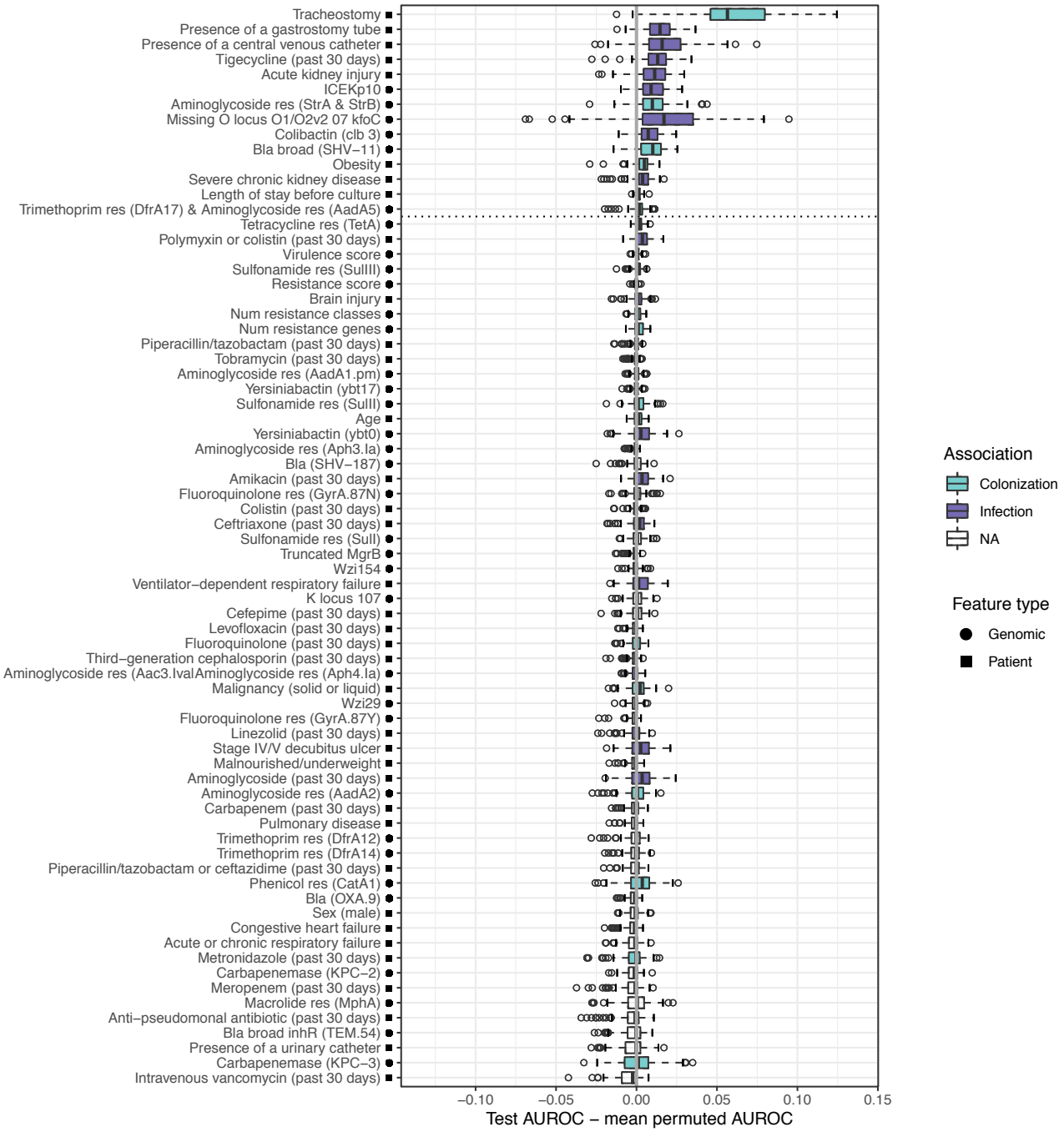

Figure S5: Differences in test vs. mean permuted AUROC across 100 data splits for each feature in the overall machine learning analysis. All features included in the model are shown. We consider features to be associated with infection/colonization if the AUROC difference is greater than zero in over 75% of the 100 data splits (see methods for more details). Features above the dotted line fall into this

867 category. The solid grey line indicates a difference of zero (i.e. the feature provides no improvement to

868 model performance). Bla=Beta lactamase, res=confers resistance to that antibiotic class.

869

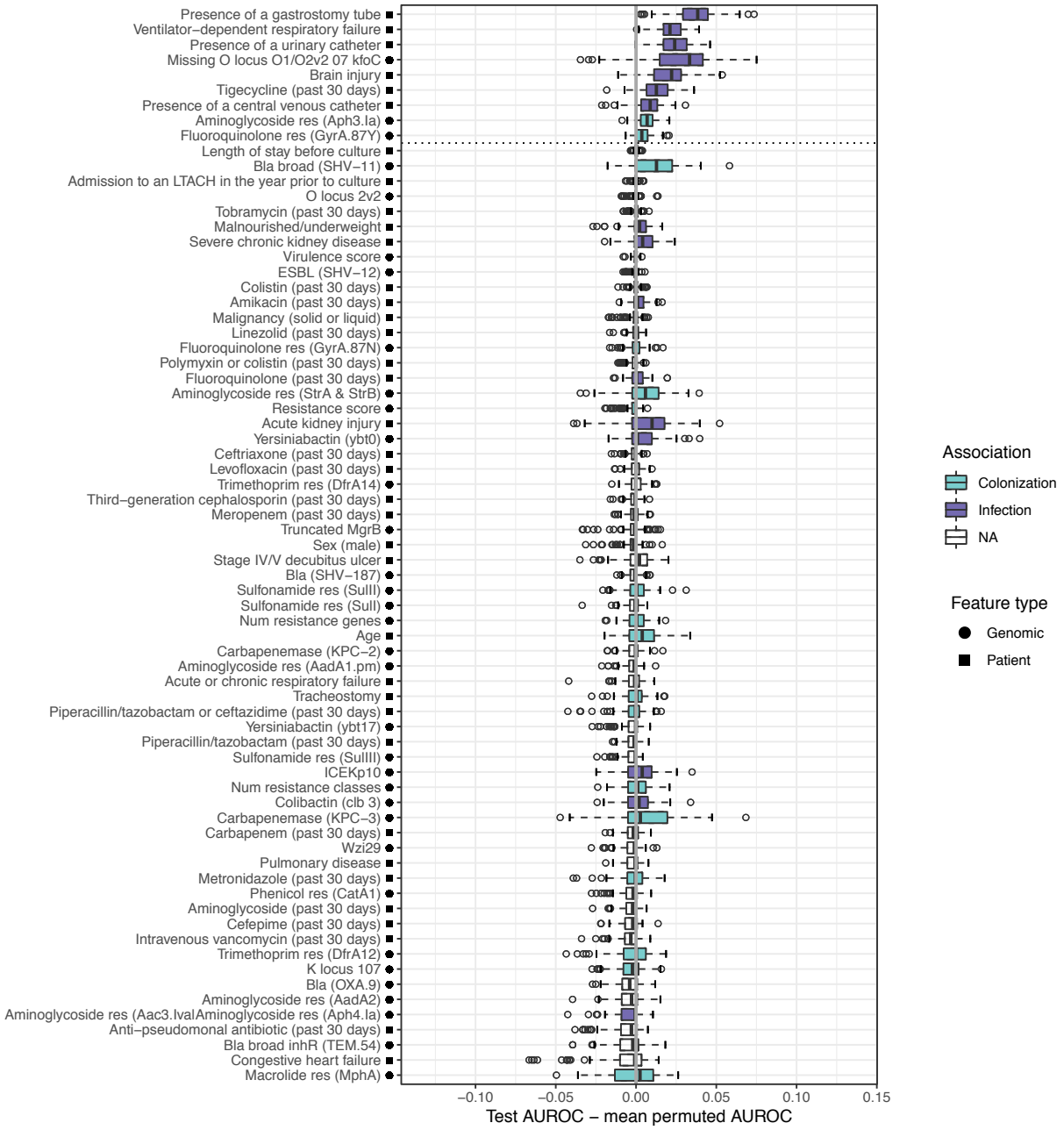

870

871 **Figure S6: Differences in test vs. mean permuted AUROC across 100 data splits for each feature in**

872 **the respiratory machine learning analysis.** All features included in the model are shown. We consider

873 features to be associated with infection/colonization if the AUROC difference is greater than zero in over

874 75% of the 100 data splits (see methods for more details). Features above the dotted line fall into this

875 category. The solid grey line indicates a difference of zero (i.e. the feature provides no improvement to

876 model performance). Bla=Beta lactamase, res=confers resistance to that antibiotic class.

877

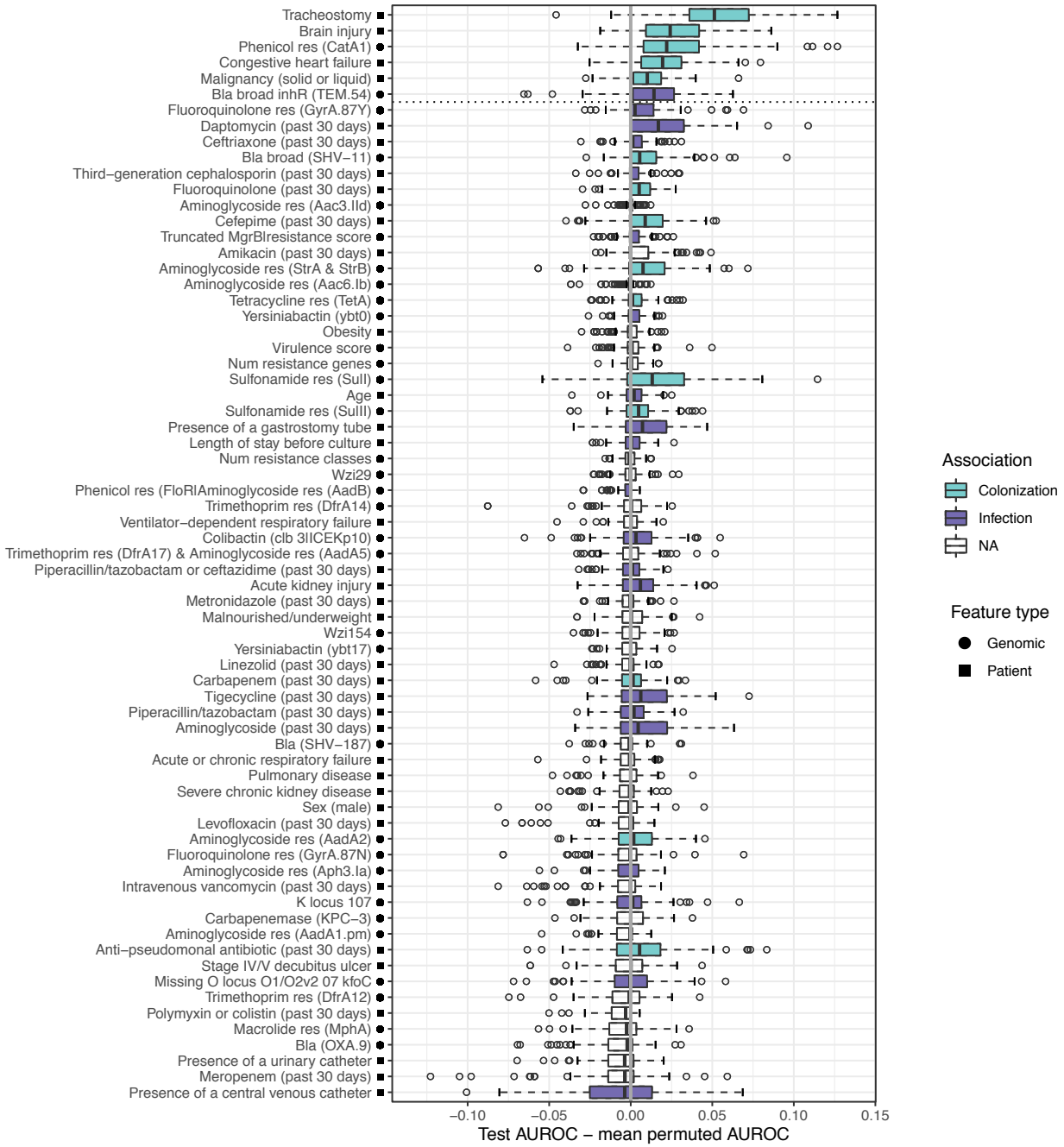

878

879 **Figure S7: Differences in test vs. mean permuted AUROC across 100 data splits for each feature in**

880 **the urinary machine learning analysis.** All features included in the model are shown. We consider

881 features to be associated with infection/colonization if the AUROC difference is greater than zero in over

882 75% of the 100 data splits (see methods for more details). Features above the dotted line fall into this
883 category. The solid grey line indicates a difference of zero (i.e. the feature provides no improvement to
884 model performance). Bla=Beta lactamase, res=confers resistance to that antibiotic class.
885

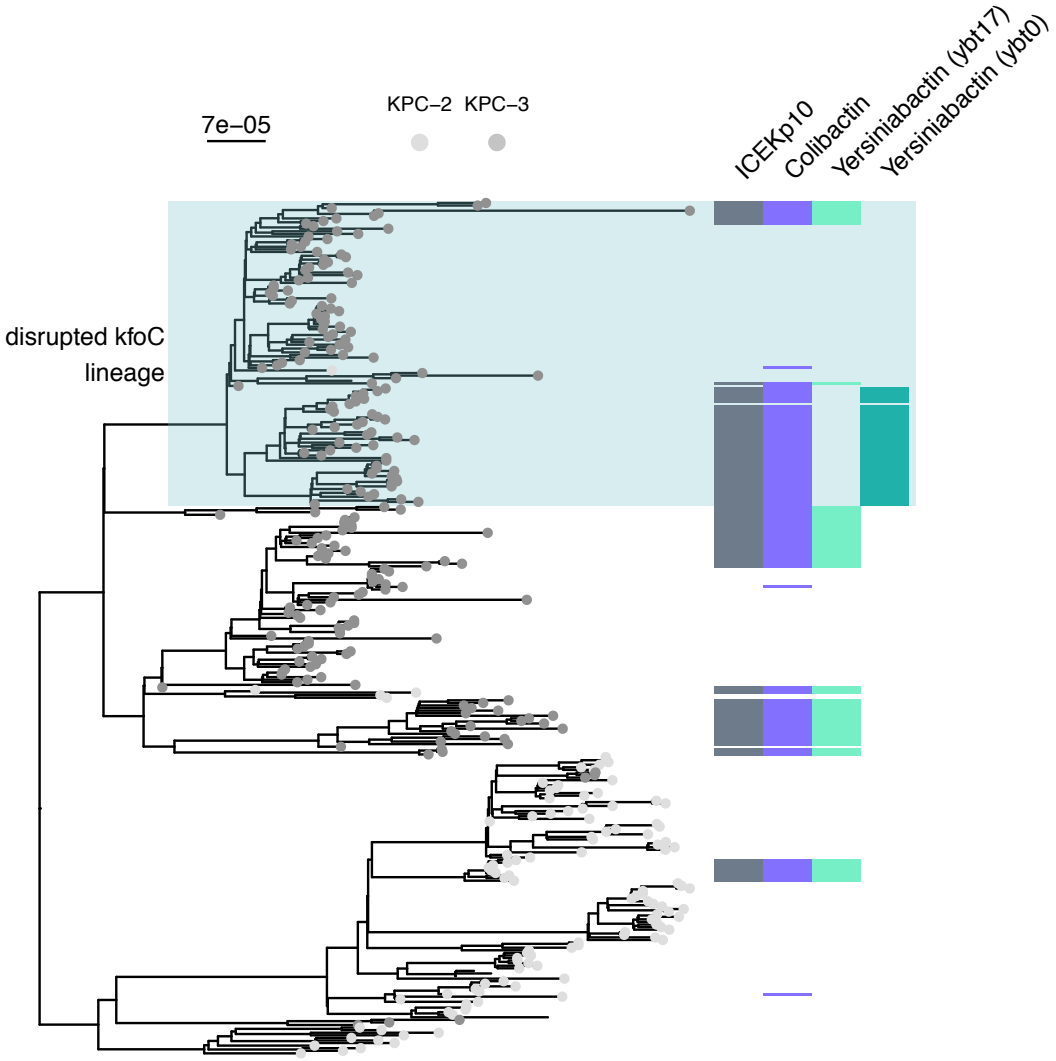

886
887 **Figure S8: Presence/absence of genomic variants on the ICEKp10 element.** The heatmap beside the
888 ST258 phylogeny indicates variant presence/absence in a given isolate. Color indicates presence and
889 white indicates absence. The scale bar above the phylogeny shows the branch length in substitutions per
890 site.
891

892

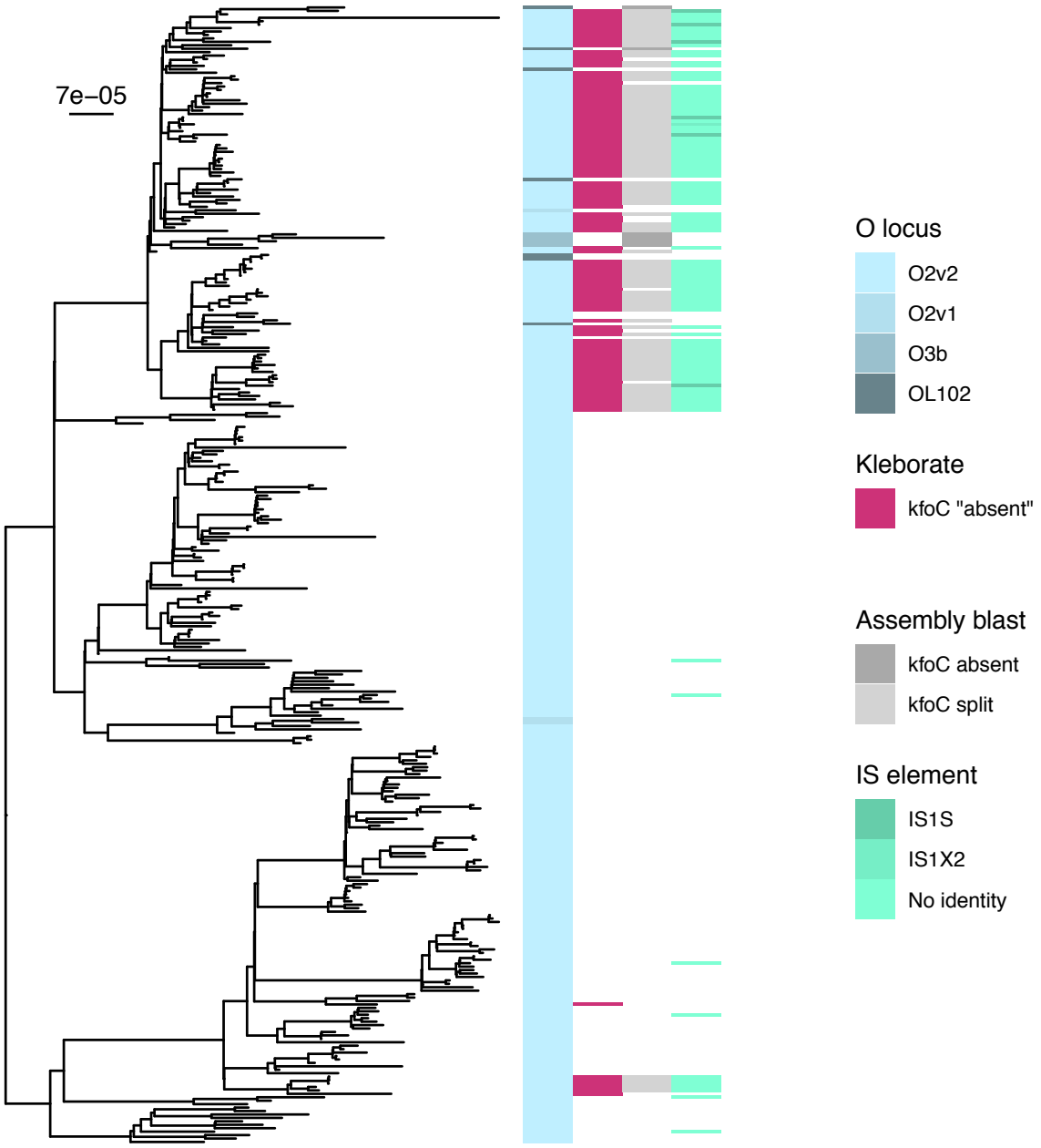

893

894 **Figure S9: kfoC contains an IS element in a subset of ST258 isolates.** The heatmap beside the
895 ST258 phylogeny indicates information about the isolate (left to right): the O locus type identified by
896 Kleborate (i.e. the curated genomic data), if Kleborate identified kfoC as missing, blast results for kfoC
897 against the genome assemblies (split between 2 assemblies or entirely absent; white indicates that kfoC
898 was intact), and IS elements identified in kfoC (white indicates no IS element detected). The scale bar to
899 the top left of the phylogeny shows the branch length in substitutions per site.

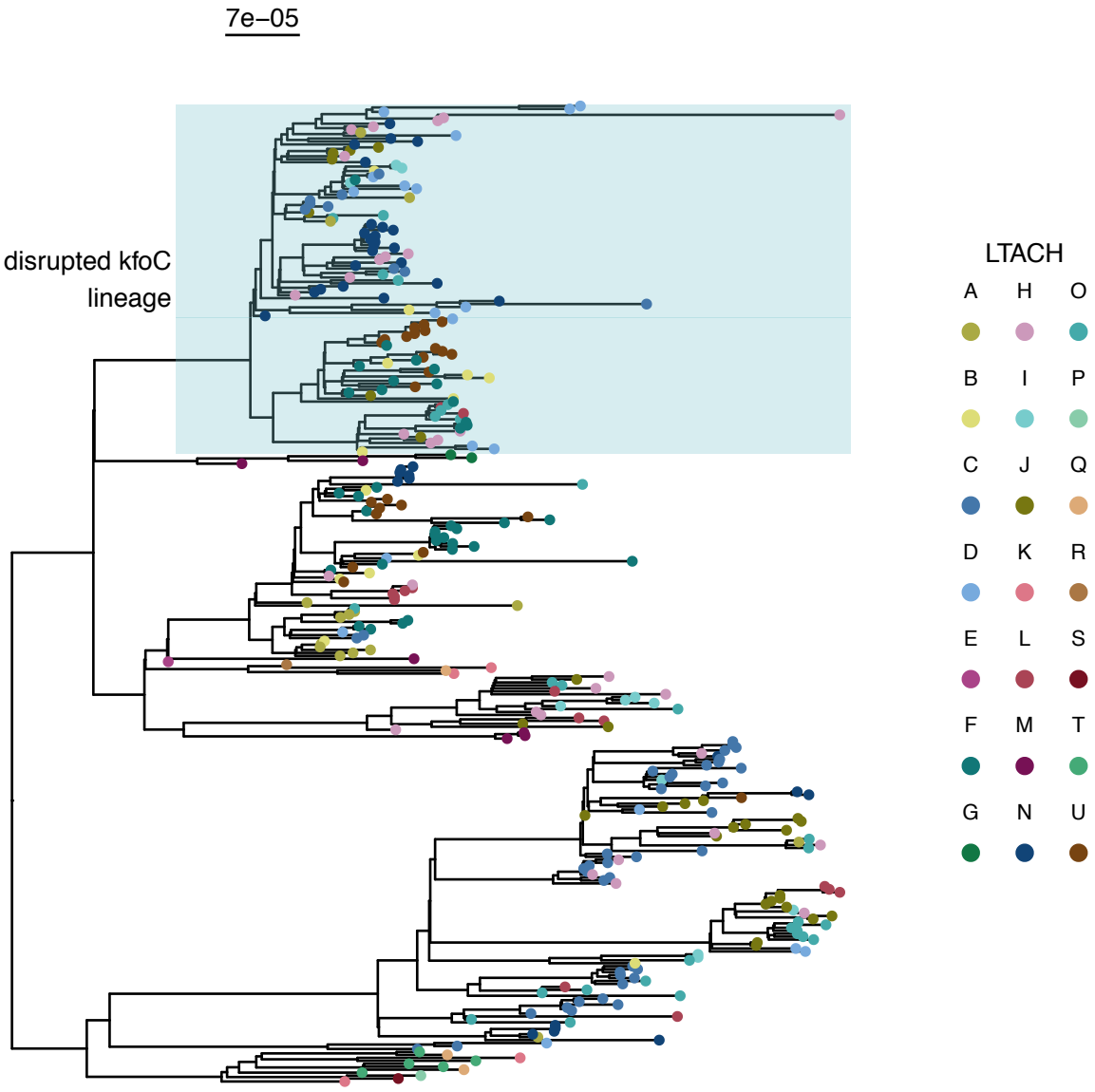

Figure S10: Isolates from different LTACHs are distributed across the phylogeny. Phylogeny of isolates indicating the LTACH the patient was in when the isolate was obtained. Isolates from several LTACHs are present in the disrupted kfoC lineage or the ybt0 lineage, and isolates from these LTACHs are not confined to those lineages. The scale bar above the phylogeny shows the branch length in substitutions per site.

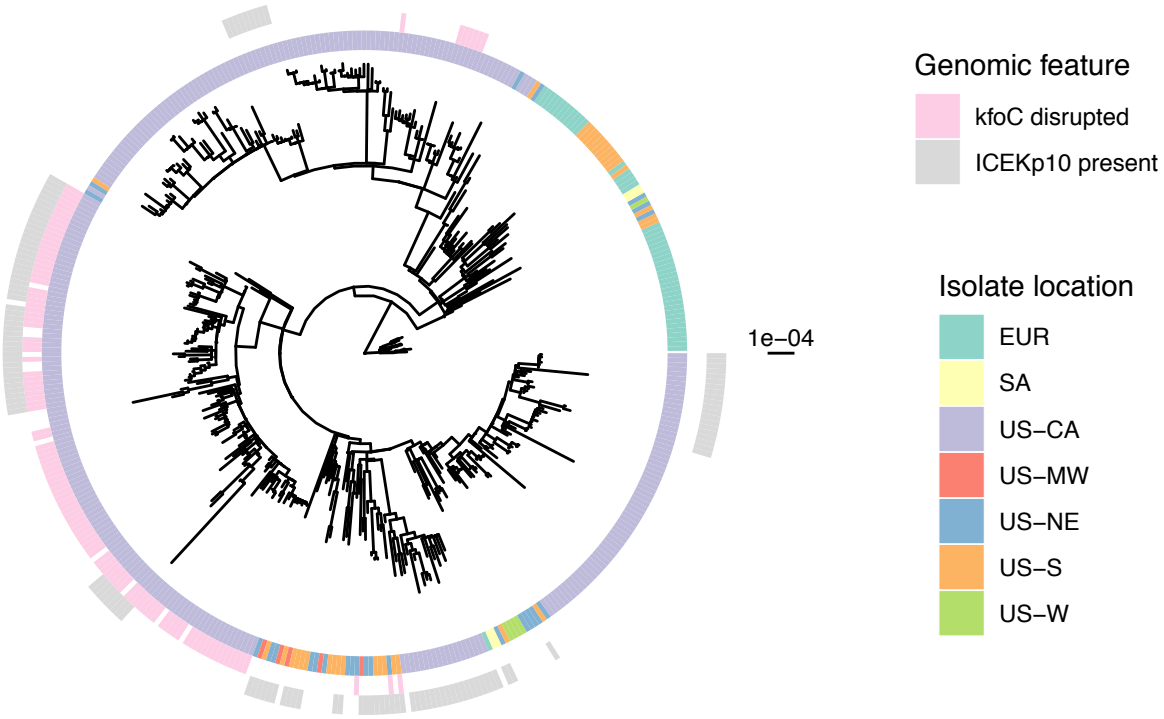

907

908 **Figure S11: Isolates containing both disrupted kfoC and ICEKp10 are mainly confined to one**
909 **ST258 clade.** Phylogeny of California LTACH isolates (US-CA) in the context of public isolates from
910 various locations (EUR=Europe, SA=South America, US-MW=US Midwest, US-NE=US Northeast, US-
911 S=US South, US-W=US West). Isolate location, as well as ybt0 presence and kfoC absence are
912 displayed for each sample. The scale bar to the right of the phylogeny shows the branch length in
913 substitutions per site.

914